ASSESSMENT OF INSECTICIDAL VIRULENCE OF PIR-LIKE TOXINS FROM *VIBRIO PARAHAEMOLYTICUS* (GAMMA PROTEOBACTERIA, VIBRIONACEAE)

by

Marilyn Amaris Mews

A Thesis Submitted to the Faculty of the

SCHOOL OF ANIMAL AND COMPARATIVE BIOMEDICAL SCIENCES

In Partial Fulfillment of the Requirements

For the Degree of

MASTER OF SCIENCE

WITH A MAJOR IN MICROBIOLOGY

In the Graduate College

THE UNIVERSITY OF ARIZONA

2020

THE UNIVERSITY OF ARIZONA

GRADUATE COLLEGE

As members of the Master's Committee, we certify that we have read the thesis prepared by Marilyn Mews, titled Assessment of Insecticidal Virulence of Pir-like Toxins from *Vibrio parahaemolyticus* (Gamma Proteobacteria, Vibrionaceae) and recommend that it be accepted as fulfilling the dissertation requirement for the Master's Degree.

_____ Date: 9/16/20

S. Patricia Stock, PhD, Thesis Director and Professor

_____ _____ Date: 9/16/20

Arun K. Dhar, PhD, Committee Chair

_____ Date: 9/21/2020

Koenraad M. Van Doorslaer, PhD, Committee Member

Final approval and acceptance of this thesis is contingent upon the candidate's submission of the final copies of the thesis to the Graduate College.

I hereby certify that I have read this thesis prepared under my direction and recommend that it be accepted as fulfilling the Master's requirement.

_____ Date: 9/1620

S. Patricia Stock, PhD

Thesis Director and Major Professor

School of Animal and Comparative Biomedical Sciences

ACKNOWLEDGEMENTS

Through my time at the University of Arizona and before, my family has always encouraged me to do my best and to achieve success. My parents and my sisters have always been and will always be my strongest supporters.

I started my journey not as a scientist but as an animal-loving future veterinarian. I volunteered at various veterinary clinics and even cared for the lions, tigers, and bears at Reid Park Zoo. Yet always there was a glimmer of science, from developing elementary science projects to questioning exactly how muscles can frame the bones to propel us forward. I was not satisfied with the "I don't know," and I had to seek it out. In college, I learned about the invisible world of microbes and my fascination was caught. Kate Johansen was the advisor who convinced me to "come to the Dark Side" and change majors from Veterinary Science to Microbiology. This journey to an Accelerated Master's in Microbiology allowed me to meet amazing teachers and mentors along the way. The first was Dr. Laura Meredith, who answered my plea to have "real lab" experience. Next came Dari Trujillo and Kyle Sharp who encouraged me to go beyond the typical and reach for a masters. This was confirmed when I had a conversation with Dr. V.K. Vishwanathan, who gave me the courage to apply to the program. After applying, I was hand-selected by Dr. Patricia Stock and Dr. Arun Dhar. I thank both for taking me on as a student. Dr. Patricia Stock's patience and guidance helped to train my mindset and critical thinking skills. She was a strong support and fostered a safe, fun working environment. It was an honor to work with her. Dr. Arun Dhar also fostered critical thinking and how to process and work out the details of the project. It was awkward at times to work in a second lab and with an unfamiliar group of people, but Dr. Dhar made sure to welcome and

support me. I would like to thank Dr. Koenraad Van Doorslaer, a member of my committee, who was also dedicated to my success.

My project came with many difficulties and challenges, as most do. Regardless, Dr. Hung Mai and Jasmine Millabas were patient as we brainstormed and experimented to get certain lab techniques to be successful. Dr. Mohammad Torabi and Dr. Mark Borgstrom graciously taught me how to analyze statistics for my project and to interpret the data. I would also like to thank Ayako Kusakabe and Rebecca Howes, members of the Stock Lab, for not only being wonderful lab supports, but also great life-long friends to lean on. Other fellow students that were first strangers and soon dear co-workers and friends were Aishwarya Rao, Mai Nguyen, and Qi Wei. We were there for each other in our ups and downs, and it made all the difference in our successes.

I have become the second person in my family to have a master's, after my grandma, and the first scientist. I am excited to be in the science field and continue to unlock the mysteries of this world with the wonderful, powerful, invisible microbes.

TABLE OF CONTENTS

LIST OF FIGURES

CHAPTER 1

CHAPTER 2

LIST OF TABLES

ABSTRACT

Vibrio parahaemolyticus Pir-like toxins are the causative agent of Acute Hepatopancreatic Necrosis Disease (AHPND) in several shrimp species. These toxins are similar to the Pir toxins produced by *Photorhabdus* bacteria, which are known to be insecticidal to a wide range of insects. Both the *Vibrio* and *Photorhabdus* Pir toxins have a binary structure with two components: Pra and Prb. Together, the two components are required to cause mortality in insects. However, it is unknown if *V. parahaemolyticus* PirAB-like toxins have insecticidal activity. Thus, the current study focused on assessing the activity of these toxins considering last instar larvae of the greater wax moth, *Galleria mellonella,* as the model organism. The effects of temperature, portal of entry, toxin concentration, and toxin source were the variables tested to assess the toxins' virulence. Infected larvae were processed for histology to observe the effect of the toxins on tissue pathology.

When comparing the two portals of entry, the toxins showed a higher insect mortality when delivered through the digestive route. Interestingly, a higher mortality was achieved at the lower concentration tested, and toxins seemed to be more virulent at 22°C. The spiracles portal of entry presented low virulence at the tested higher dose. When comparing recombinant and purified proteins from overnight cultures, a higher insect mortality was achieved with the recombinant proteins. Preliminary histology observations showed a lack or shortening of microvilli in the gut of treated larvae compared to the healthy control.

Overall, *V. parahaemolyticus* PirAB-like toxins had very low insecticidal activity in *G. mellonella* larvae. Future studies should focus on expanding the host range to other insect orders, conducting dose response assays, and assessing the effect of *in vitro* association of Pra and Prb.

CHAPTER 1: INTRODUCTION

Vibrio parahaemolyticus and Its Impact in Marine Industry

Vibrio parahaemolyticus (Gamma Proteobacteria, Vibrionaceae) is a Gram-negative, halophilic, mesophilic, and rod-shaped bacterial species that is found in estuarine and marine environments worldwide (Drake et al., 2007; Hong et al., 2016). *Vibrio parahaemolyticus* affects a wide range of marine animals, including squid, mackerel, tuna, sardines, crab, conch, shrimp, and bivalves, such as oysters, clams, and mussels (FDA, 2020). This bacterium favors warm waters above 15°C, so outbreaks typically happen in the summertime (Kaneko and Colwell, 1973; Letchumanan et al., 2014). In waters that drop below 15°C, *Vibrio* survives the winter in the sediment and is therefore undetectable. In waters that stay above 15°C, *Vibrio* can be detected year-round (Kaneko and Colwell, 1973; Karunasagar et al., 1994).

In humans, *V. parahaemolyticus* causes gastrointestinal illness if affected undercooked or raw seafood among the hosts of this pathogen is consumed (Letchumanan et al., 2014; CDC, 2019). Oysters are currently the most common carrier of *V. parahaemolyticus* infection to humans, as they are typically consumed raw (Froelich and Noble, 2016). Symptoms of infection appear about 17 h after the seafood is eaten and include abdominal cramping, nausea, vomiting, and fever (Rezny and Evans, 2019). Typically, these infections are self-regulating and are resolved within 72 h (Finkelstein, 1996). The CDC (2019) reports that from all *Vibrio* species, there are approximately 80,000 cases, 500 hospitalizations, and 100 deaths each year in the United States.

Two hosts of *V. parahaemolyticus*, in particular, are the shrimp *Penaeus vannamei* and *Penaeus monodon* (Letchumanan et al., 2014). *Vibrio parahaemolyticus* is part of the shrimp's natural gut flora; however, certain strains of this bacterium trigger Early Mortality Syndrome (EMS) in shrimp. EMS causes nearly 100% mortality within 20 to 30 days of a pond's stocking

with shrimp post-larvae (Hong et al., 2016; Li et al., 2017). The name of this disease was later changed to Acute Hepatopancreatic Necrosis Disease (AHPND) in reference to the targeted organs and pathology. Recently, the disease has been detected in *Marsupaneus japonicus* although the susceptibility of *M. japonicus* is yet to be confirmed (OIE, 2020).

The first outbreak of AHPND was reported in China in 2009 and spread to shrimp farms around the world, causing approximately $1 billion in industry losses a year (Nunan et al., 2014; Hong et al., 2016). There is currently no treatment for AHPND, but certain preventative measures can be conducted, such as maintaining proper stocking density and regular pond cleaning (OIE, 2019; GAA, 2020). This disease has serious implications in the shrimp industry which is the most valuable traded marine product in the world today, estimating a value of $45 billion, and continues to grow at approximately 10% annually. China and Thailand account for nearly 75% of the global shrimp production (FAO, 2020).

Acute Hepatopancreatic Necrosis Disease

The hepatopancreas of juvenile shrimp is affected by AHPND (Tran et al., 2013). This organ has similar function to the liver and pancreas in mammals. It secretes enzymes for food digestion and stores and releases lipids for supplying energy for molting and reproduction (Gibson and Barker, 1979). AHPND infection has been described as a two-stage process with an acute phase followed by a terminal phase. During the acute phase, the hepatopancreas tubule epithelial cells detach from the basement membrane and get sloughed into the tubule lumen. Bacteria are not readily visible in this stage (Tran et al., 2013; Han et al., 2015). At the terminal phase, the hepatopancreas is colonized with bacteria and hemocyte aggregations are seen at the histological level. Shrimp then die from a malfunctioning hepatopancreas or secondary bacterial infections

(Tran et al., 2013; Han et al., 2015). Recently, a third phase of AHPND infection, a chronic phase, has been reported in certain AHPND-tolerant *P. vannamei* shrimp (Aranguren Caro et al., 2020). In the chronic phase, melanized granuloma and hemocytic nodules in the hepatopancreas that resembles septic hepatopancreatic necrosis (SHPN) are observed (Aranguren Caro et al., 2020).

Figure 1 shows a shrimp affected with AHPND (A) at a macro-level (top image) and at the hepatopancreas' histological level (bottom image). A healthy shrimp is displayed to the right (B) to show the differences between the healthy shrimp and the unhealthy shrimp (Restrepo et al., 2018). In 2015, novel proteins with toxic activity were found in *V. parahaemolyticus* in connection to AHPND (Han et al., 2015; Lee et al., 2015). These AHPND-causing toxins are similar to *Photorhabdus* insect related (Pir) toxins and are thus referred to as Pir-like (see section below).

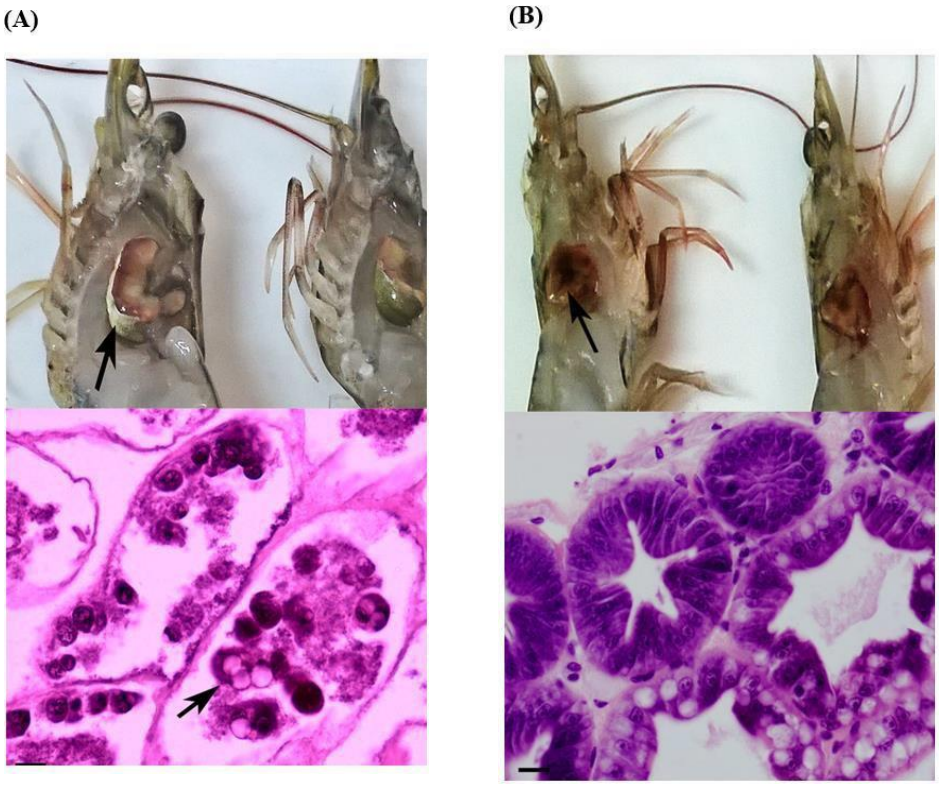

Figure 1. AHPND in *P. vannamei.* **(A)** Top image shows a sick AHPND-diagnosed shrimp displaying a pale hepatopancreas (black arrow). Bottom image shows the cell damage and tubule necrosis of the sick shrimp's hepatopancreas (hematoxylin and eosin (H&E) stained). **(B)** Top

image shows a healthy shrimp with a dark-colored hepatopancreas (black arrow). Bottom image shows healthy shrimp hepatopancreas tissue (H&E stained). Images from Restrepo et al. (2018).

V. parahaemolyticus Toxins and Virulence Factors

Vibrio parahaemolyticus produces various virulence factors that have been shown to play a role in AHPND (Park et al., 2004; Li et al., 2017). They are primarily produced and released by Type III Secretion Systems (T3SS), which are known to play a key role in the toxicity of *V. parahaemolyticus* delivering effector proteins into the host cell to modulate host cell functions. The secretion structure consists of a main portion that spans both the inner and outer bacterial membranes and a syringe-like apparatus that injects the effector proteins directly into the eukaryotic host cell (Tseng et al., 2009; Izore and Dessen, 2011).

Two T3SS gene clusters have been found in the genome of this bacterium (Broberg et al., 2011; Wagley et al., 2018). The first T3SS (T3SS1) is present in all *Vibrio parahaemolyticus* strains and releases effectors proteins, VopQ, VopR, VopS, and VPA0450, that cause cytoxicity and apoptosis in HeLa cells (Park et al., 2004; Burdette et al., 2008; Broberg et al., 2010). The second T3SS (T3SS2) is present in clinical *V. parahaemolyticus, V. cholerae, V. hollisae,* and *V. mimicus* strains and releases the effector proteins VopA, VopC, VopL, and VopT. These proteins cause cytotoxicity in human cultured cells (Park et al, 2004; Okada et al., 2010; Kodama et al., 2010). T3SS2 also produces thermostable direct haemolysin (*tdh*) and TDH-related haemolysin (*trh*) toxins in *V. parahaemolyticus,* which can cause gastroenteritis in humans together or separately (Wagley et al., 2018). The effects of these toxins have not been tested in shrimp.

The Type 6 Secretion System (T6SS) is thought to be involved in the secretion of Pir-like proteins, a recently discovered toxin that is the causative agent of AHPND (Han et al., 2015; Lee et al., 2015; Li et al., 2017). T6SS are induced in high-salt environments when temperatures are

high and surface sensing is activated by dense bacterial populations. Li et al. (2017) found that all of the tested AHPND-causing strains of *Vibrio parahaemolyticus* contained the T6SS; whereas, none of the non-AHPND causing strains contained the T6SS. The T6SS genes were also found in other AHPND-causing *Vibrio* species, including *Vibrio owensii* and *Vibrio campbellii* (Li et al., 2017).

Pir-like Toxins

Han et al. (2015) discovered Pir-like toxins in *Vibrio parahaemolyticus* strain 13-028/A3 in a 69kb plasmid, pVA1. These toxins were named after *Photorhabdus* insect related toxins (Pir) toxins, which were first discovered in *Photorhabdus* (Gamma Proteobacteria, Enterobacteriaceae) (Ffrench-Constant et al., 2000). *Photorhabdus* is a bioluminescent, gram-negative bacilli and is an insect pathogen (Waterfield et al., 2009). The bacteria live symbiotically in the intestine of infective juvenile nematodes of the genus *Heterorhabditis* (Nematoda, Heterorhabditidae), which are responsible for vectoring the bacteria from one insect host to the other (Boemare et al., 1993; Forst et al., 1997). *Photorhabdus* produces four main toxins: Mcf (Make caterpillars floppy), PVCs (Photorhabdus Virulence Cassettes), Tc (Toxin Complexes), and Pir toxins (Duchaud et al., 2003).

Pir toxins have a binary structure with two components, Pra and Prb, which are the products of two loci, plu4093/4437 and plu4092/4436 respectively (Waterfield et al., 2005). The toxins were found to have lethal capabilities against a wide range of insects. Both components are required to cause mortality in insects and therefore be insecticidal (Waterfield et al., 2005; Ahantarig et al., 2009). Various studies have shown that Pir toxins have either oral or injectable virulence in multiple insect species including *Spodoptera exigua, Aedes albopictus, Aedes*

aegypti, *Plutella xylostella*, and *Galleria mellonella* (Waterfield et al., 2005; Blackburn et al., 2006; Ahantarig et al., 2009; Li et al., 2014).

Under histological analysis, Pir toxins were found to cause cytotoxicity, damage to midgut epithelial cells, and shedding and swelling of the apical gut membranes within *Plutella xylostella* larvae (Figure 2; Blackburn et al., 2006).

Li et al. (2014) demonstrated the cytotoxic effects of Pir toxins on insect CF-203 midgut cells (Figure 3). Specifically, the authors showed that application of purified Pra/Prb protein mixture caused loss of viability of the midgut cells after 24 h of incubation. Moreover, cells treated with Pra/Prb displayed morphological changes typical of apoptosis, including cell shrinkage, cell membrane blebbing, nuclear condensation, and DNA fragmentation (Li et al., 2014).

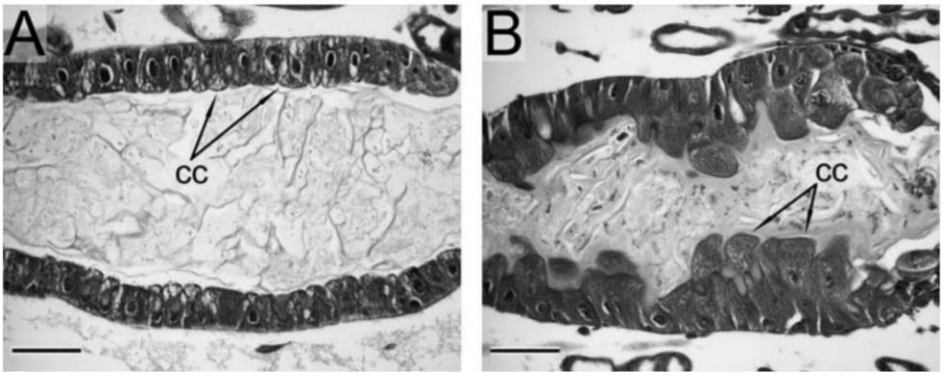

Figure 2. Histology of *Plutella xylostella* larvae fed with *E. coli* containing *pir* genes. **(A)** Empty pGEM vector showing healthy columnar cells (CC). **(B)** pGEM-Pra/b showing apical swelling of CC. Both A and B show the most posterior region of the midgut, adjacent to the hindgut. Scale bars = 50 um. Images from Blackburn et al. (2006).

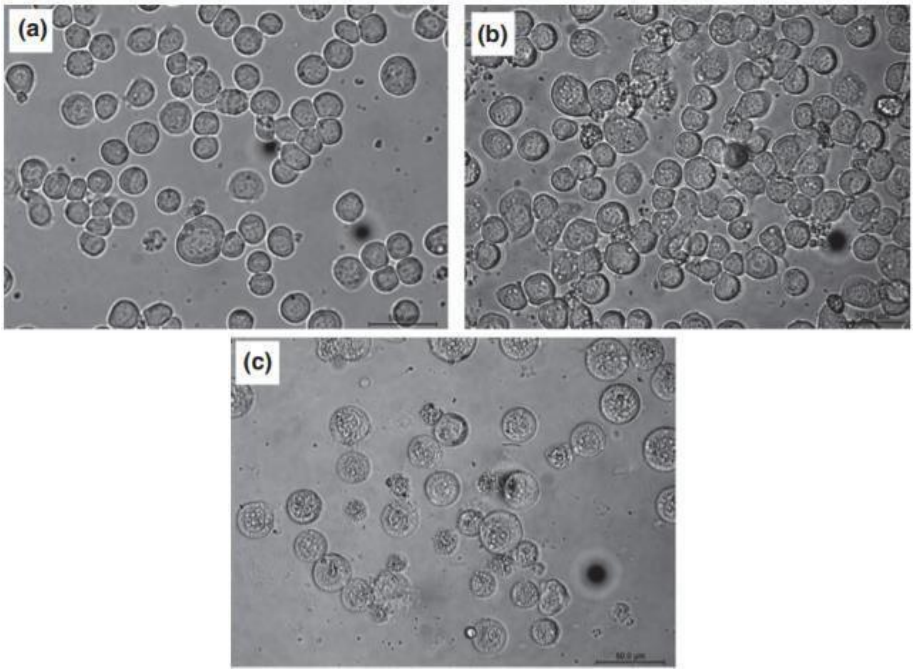

Figure 3. PirAB-treated CF-203 cells from *Choristoneura fumiferana* larvae. **(A)** Treatment with deionized water (negative control). **(B)** Treatment with 0.2 µM Prb alone for 24 h. **(C)** Treatment with 0.1 µM of Pra/Prb mixture for 24 h. Images from Li et al. (2014).

Similar to *Photorhabdus*, *V. parahaemolyticus* Pir-like toxins are also binary and therefore have two components: Pra and Prb. Because of their similarity to *Photorhabdus* Pir toxins, these *Vibrio* toxins are often referred to as "Pir-like." As indicated before, these toxins have been shown to cause AHPND in shrimp (Lee et al., 2015).

Both *Photorhabdus* and *Vibrio* PirAB affect the organs of the digestive tract (midgut and hepatopancreas) of their hosts. *Photorhabdus* Pir toxins cause mortality through either the oral or the hemolymph injection route in insect larvae (Waterfield et al., 2005; Ahantarig et al, 2009). *Vibrio* PirAB-like proteins cause mortality through the oral route as well (Lee et al., 2015).

The histopathology of digestive organs affected by these toxins is also similar. According to Blackburn et al. (2006), the posterior midgut of insects is most severely affected by Pir toxins. The columnar midgut epithelial cells swell and shed their apical membranes into the gut lumen

(Blackburn et al., 2006; Li et al., 2017; Restrepo et al., 2018). Similarly, *Vibrio* Pir-like toxins cause the hepatopancreas tubule epithelial cells to detach from the basement membrane and slough into the tubule lumen (Tran et al., 2013; Han et al., 2015).

When looking at amino acid sequence similarity, Han et al. (2015) found that similarity between *Photorhabdus* Pir and *Vibrio* Pir-like toxins is low for both the Pra and Prb components (between 28 to 35%). Table 1 summarizes the comparisons between *Photorhabdus* PirAB and *Vibrio* PirAB-like toxins.

Table 1. Comparison summary between *Photorhabdus* PirAB and *Vibrio* PirAB-like toxins

	Photorhabdus PirAB	*Vibrio* PirAB-like
Amino Acid Sequence Similarity to Each Other	Pra: 28 - 35% Prb: 28 - 31%	
Mode of Action	Midgut epithelial cells at the apical membrane swell, detach, and shed into the gut lumen	Hepatopancreas epithelial cells at the basement membrane detach and slough into the tubule lumen
Targeted Organs	Digestive System, Hemolymph	Digestive System

Since the pVA1 plasmid encoding the *Vibrio* binary toxins can be transferred to different bacterial species, it has been speculated that the *Vibrio* plasmid containing the *pir* toxin genes was passed to the *Photorhabdus* species (Han et al., 2015). This is plausible since *Photorhabdus* are the only known group of terrestrial, bioluminescent bacteria, and bioluminescence in bacteria is usually only found in marine environments (Vlisidou et al., 2019; Tanet et al., 2019). In this respect, it has been speculated that *Photorhabdus* bacteria began in a marine environment and in that time, a *Vibrio* species may have transferred the Pir-encoding plasmid to a *Photorhabdus* bacteria, thus passing *pir* genes and toxins to them (Kondo et al., 2014).

It has also been hypothesized that the pVA1 plasmid can be transferred to other *Vibrio* species, as Pir-like toxins have been found in other *Vibrio* species, including *Vibrio campbellii* from Vietnam and *Vibrio ownesii* in China (Han et al., 2015). Studies have shown that any *Vibrio* species that express the Pir-like toxins can cause AHPND in shrimp (Li et al., 2017, Han et al., 2017). Various studies demonstrated *Vibrio* AHPND-causing spp. harbor plasmids that contain the *pra* and *prb* toxin genes that are homologs of the *Photorhabdus* insect-related (Pir) binary toxins (Liu et al., 2003; Kondo et al., 2015; Lee et al., 2015; Dong et al., 2017; Restrepo et al., 2018). According to Kondo et al. (2014), this plasmid is carried by all AHPND-causing strains of *Vibrio*. However, some non-pathogenic strains of *Vibrio* also carry the pVA1 plasmid, suggesting that although the plasmid is present, the binary toxin gene is absent (Kondo et al., 2014; Kanrar and Dhar, 2018).

Amino acid sequence similarity between *V. parahaemolyticus* and *V. campbellii* Pir toxins is high, ranging from 99 and 100% similar to Pra and Prb, respectively. The dendrogram shown in Figure 4 was built from available toxin sequences in GenBank and graphically demonstrates the two *Vibrio* species clustering together for both Pra and Prb.

PirAB toxins have a high similarity among *Photorhabdus* strains and species. For example, *P. asymbiotica,* Pra has 86% similarity to *P. luminescens*; whereas, Prb is 94% similar (Ahantarig et al., 2009). The high similarity within *Photorhabdus* species suggests that these toxins may have been horizontally transferred (Han et al., 2015). The dendrogram demonstrates the two *Photorhabdus* species clustering together for both Pra and Prb (Figure 4).

Pir-like toxins have been discovered in other Gamma-Proteobacteria, such as *Yersinia*and *Xenorhabdus* which are known to have insecticidal activity (Duchaud et al., 2003; Hao et al., 2019). *Xenorhabdus* is an entomopathogenic bacterium with a very similar life cycle to

Photorhabdus. Analysis of the genome of this bacterium showed the presence of gene homologs for Pir toxins (Yang et al., 2017). Specifically, the predicted amino acid sequences of Pra and Prb in the genome of *Xenorhabdus beddingii* showed 58% and 51% similarity with the sequences from *Photorhabdus.* However, when compared to *V. parahaemolyticus* toxins, the sequence similarities ranged between 28.5 and 30.9% for Pra and Prb, respectively (Appendix A).

Yersinia intermedia has been isolated from freshwater sources and animals, such as oysters and shrimp (Martin et al., 2009). Many *Yersinia* spp. cause diarrheal disease in humans; however, *Y. intermedia* has rarely been detected in stools and does not seem to play a role in diarrheal disease (Punsalang et al., 1987). Analysis of the genome of this bacterium showed the presence of gene homologs for Pir toxins (Duchaud et al., 2003). Specifically, the predicted amino acid sequence of Pra and Prb in the genome of *Yersinia intermedia* showed 45% and 48% similarities with the sequences from *Photorhabdus.* However, when compared to *V. parahaemolyticus* toxins, the similarities ranged between 29.4 and 37% for Pra and Prb, respectively (Appendix A).

The structure of the Prb component in *V. parahaemolyticus* has been compared to Cry2Aa toxins produced by another insect pathogenic bacterium, *Bacillus thuringiensis* (Bt). Although their amino acid sequence similarities are low, resulting in 16.7% similarity for 51% of sequence coverage, these toxins have similar structural topology and have thus been compared (Appendix A; Lee et al., 2015; Lin et al., 2019).

Similarly, Pir toxins have been paralleled to the juvenile hormone esterase (JHE) produced by the Colorado potato beetle, *Leptinotarsa decemlineata* (Vermunt et al., 1997, Duchaud et al., 2003, Waterfield et al, 2005). This protein is responsible for initiating metamorphosis in this beetle. If this protein is not hydrolyzed, the insect remains in the larval stage (Crosland et al., 2005). Interestingly, when *Photorhabdus* PirAB proteins were discovered,

they were termed “JHE-like” due to their sequence similarity with JHE. However, research done by Waterfield et al. (2005) showed that PirAB does not cause metamorphosis in insects (Waterfield et al., 2005). Sequence identity between *V. parahaemolyticus* Pir-like toxins and JHE is also low. With a 70% coverage, the similarity to Pra is only 28%; whereas, Prb has 24.6% similarity to JHE with a 90% coverage (Appendix A).

(A)

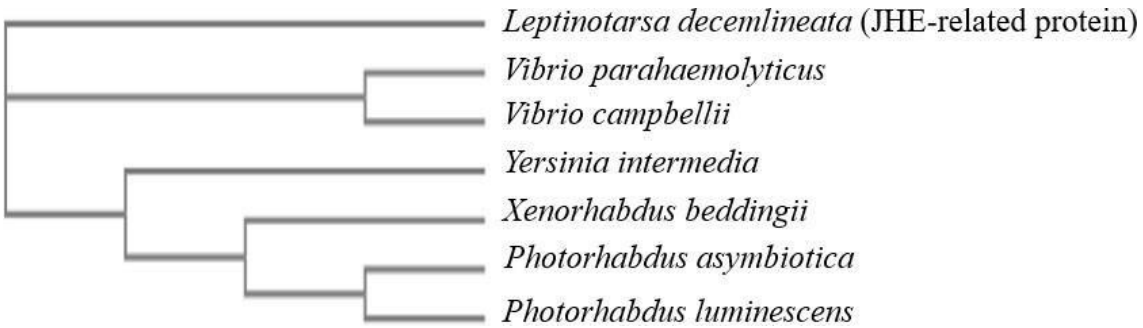

(B)

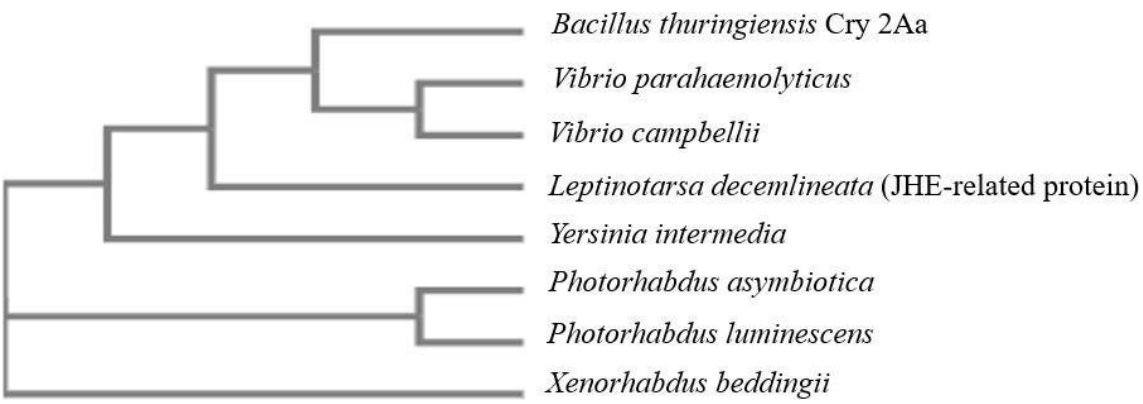

Figure 4. Dendrogram of *V. parahaemolyticus* **(A)** Pra and **(B)** Prb toxins and other related proteins.

Hypothesized Mechanism of Action for Pir-like Toxins

The specific mechanisms of how Pir proteins operate, attach to host cells, and cause disease are not known. The Pra and Prb components are secreted by *Vibrio* during the mid-log phase and

upon translation, the two components interact (Lee et al., 2015). They can also interact *in vitro* to form a Pra/Prb complex (Lee et al., 2015). Lin et al. (2019) proposed that both components form a heterotetramer, making the ratio of Pra to Prb 2:2. Building on the structural similarity between Prb and the Cry toxins of *Bacillus thuringiensis* (Bt), Lin et al. (2017) compared the crystal structures of Pir-like toxins in *Vibrio parahaemolyticus* (Figure 5A) to Bt Cry toxins.

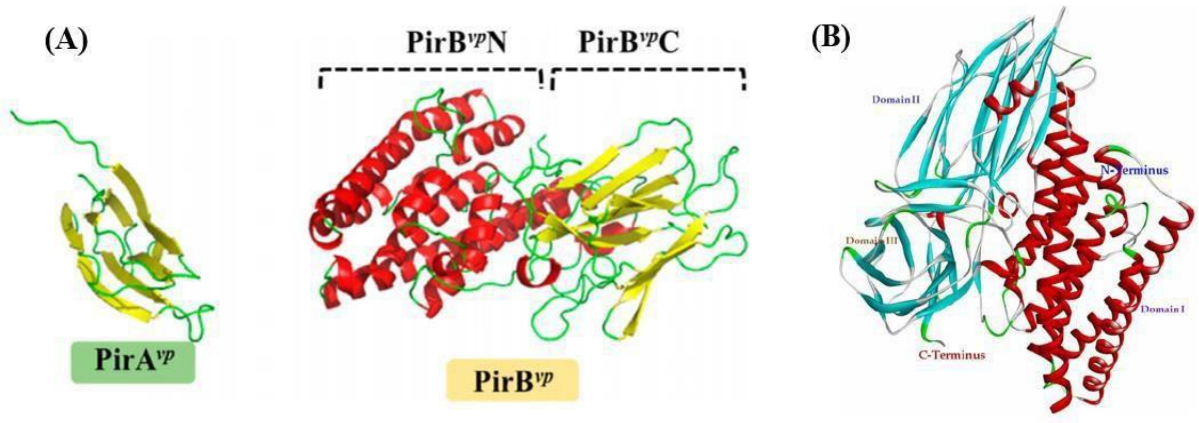

Figure 5. Crystal structures of **(A)** *Vibrio parahaemolyticus* Pra (left) and Prb (right) and **(B)** *Bacillus thuringiensis* Cry toxin. Image from Lin et al. (2017).

Bt Cry toxins consist of three domains: Domain I, Domain II, and Domain III (Figure 5B). Domain I is pore-forming and is the likely function of the Prb N-terminus (Figure 6A). Cry Domain II is the receptor binding portion of the molecule, which is likely the function of the Prb C-terminus (Figure 6C). Cry Domain III is the docking part of the toxin that binds to the receptor on the cell surface (Figure 6D). Cell docking via receptor binding is likely the mechanism of Pra. Although it is not known which receptor Pra binds to, it is hypothesized to either bind to N-acetylgalactosamine (GalNAc), which is the receptor that Cry Domain III binds to, or an oligosaccharide, due to a unique sugar-binding region formed by three loops in Pra (Figure 6E; Lin et al., 2017).

By comparing PirAB-like toxins to Bt Cry toxins, it could be speculated that *V. parahaemolyticus* Pir-like toxins likely work by Pra first docking to the host cell and then Prb delivering the toxin (Lin et al., 2017). To narrow the toxins' specific mode of action, the N-terminus of Prb has a hydrophobic center (Figure 6B). Therefore, there is likely a conformational change in the toxin when it binds to the receptor, allowing the toxin molecule to "flip" and interact with different membrane lipids in the host cell. This mechanism is known as the "Inside-Out Membrane Fold" (Lin et al., 2017).

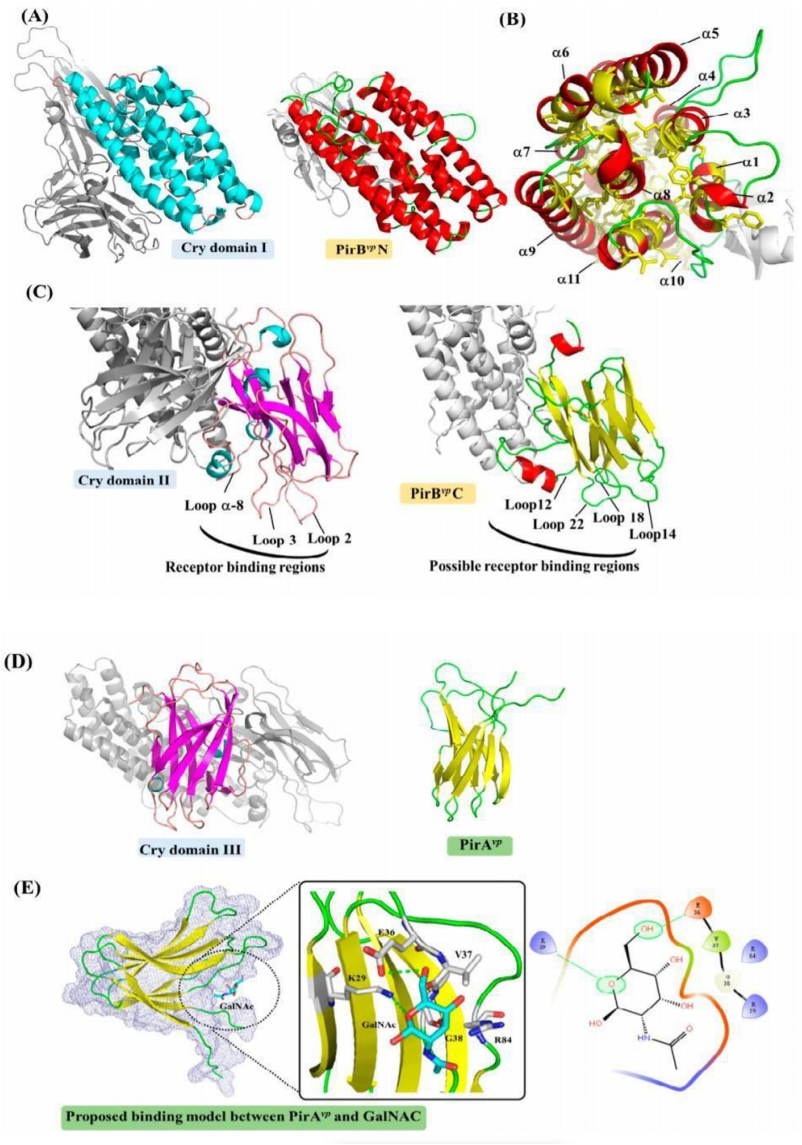

Figure 6. (A) Similarities between Cry Domain I (left) and *Vibrio* Prb N-terminus (right). **(B)** Close-up of the hydrophobic center of Prb N-terminus. **(C)** Structural comparison of Cry Domain II (left) and Prb C-terminus (right). **(D)** Structural comparison of Cry Domain III (left) and *Vibrio* Pra (right). **(E)** Proposed binding model between GalNAC (the binding receptor for Bt) and *Vibrio* Pra. Images from Lin et al. (2017).

Vibrio Pir-like Toxins and Their Potential in Insect Pest Management

Productivity of crops is severely hindered by unmanaged pests (Oerke, 2006). Approximately $56 billion are spent annually world-wide on pesticides, and $9 billion of that is spent in the United States alone, totaling 16 to 18% of the total expenditure on pesticides (EPA, 2012). Most chemical pesticides have adverse effects to humans and animals, including carcinogenic and neurotoxic (Pimentel et al., 2005). They also impact the environment including groundwater, soil, etc. (Pimentel et al., 2005). Thus, alternatives to chemical pesticides, such as bio-pesticides, are actively sought. Bio-pesticides involve living organisms, such as natural enemies or microbial organisms and/or their byproducts. They are harmless to humans and animals, including wildlife, and they do not pollute soil or groundwater (Pimentel et al., 2005; Oerke, 2006). In addition to their increased ecological safety, bacterial biopesticides typically have a specific host range (EPA, 2016).

While the chemical pesticide market grows approximately 1 to 2% a year, the microbial pest control market grows 10% annually (Koul, 2011). Bacteria-derived pesticides represent about 75% of the current market of biopesticides. One family of bacteria in particular that produces insecticidal toxins are Enterobacteriaceae. The gram-negative bacteria within this genus that produce insecticidal toxins are *Yersinia, Serratia, Xenorhabdus,* and *Photorhabdus* (Castagnola and Stock, 2014). The most widely used biopesticide is Cry toxin and it comes from

the bacteria, *Bacillus thuringiensis* (Bt) (Ibrahim et al., 2010; Paramasiva et al., 2014; EPA, 2020).

Among microbial organisms, several bacterial species have successfully been implemented in pest management, including *Bacillus thuringiensis*, *Bacillus subtillis*, and baculoviruses (Palma et al., 2014; Wang et al., 2018; Rohrmann, 2019). *Bacillus thuringiensis* (Bt) produces several toxins, including Cyt, Vpa, Vpb, Vip, and Cry. Cyt proteins are endotoxin crystals that are mainly toxic against mosquitoes and black flies (Palma et al., 2014). Vpa and Vpb toxins are binary proteins that need each other to act. Vip does not share sequence similarity to Vpa or Vpb and has a different mechanism of action and binding place than from the Cyt and Cry toxins (Chakroun et al., 2016). Cry toxins are endotoxin crystals that activate within the alkaline pH of the insect gut. The crystals have been shown to effectively kill various species from diverse orders including Lepidoptera (i.e. pink bollworm, etc.), Coleoptera (i.e. beetles, white grubs), and Diptera (i.e. mosquitos) (Höfte and Whiteley, 1989; Palma et al., 2014). An important characteristic of Bt use as a biopesticide is its spore development because then it can persist in the environment for long periods of time (Castagnola and Stock, 2014).

Over time, certain insects became resistant to Cry toxins (Head et al., 2010). Strategies to overcome Bt Cry toxin resistance have considered non-Bt, susceptible refugia planted among Bt crops (Head et al., 2010). In Arizona, the pink bollworm, *Pectinophora gossypiella* (Lepidoptera: Gelechiidae) was completely eradicated from the cotton crop using the plant refuge strategy and transgenic plants (USDA, 2018).

Another strategy to prevent Bt resistance has considered the pyramiding of toxins, where combinations of toxins with different modes of action and host range are used to swiftly overwhelm the insect immune system and delay resistance (Roush, 1998; Mehrotra et al., 2011;

Chakroun et al., 2016). Once such combination with the Cry toxins is the Vip toxin. Vip does not share sequence similarity, mechanism of action, or binding location to Cry toxins, so Vip has been used in combination with Bt and employed on maize and cotton crops (Zhao et al., 2003; Zhao et al., 2005; Chakroun et al., 2016).

To combat insect resistance to microbial biopesticides, the search for novel bacterial species and/or strains that produce insecticidal toxins are actively being sought. These new toxins may target different insects and provide specific inhibition against harmful pests. In this respect, the present study focused on the examination of *V. parahaemolyticus* Pir-like toxins insecticidal activity as a prospect for insect pest management.

Galleria mellonella as a Model Organism

The greater wax moth *Galleria mellonella* (Linnaeus) is a member of the Pyrallidae in the order Lepidoptera. This insect has a worldwide distribution and is known for its parasitism and destruction of *Apis mellifera* and *Apis cerana* honeybee hives (Paddock, 1918; Kwadha et al., 2017). When *G. mellonella* infect a honeybee population, they feed on the wax comb, pollen, honey, and bee skin casts (Shimanuki, 1980). The bees' resources are squandered, and the hive becomes more susceptible to other infections from bacteria and/or predators (Kwadha et al., 2017).

The greater wax moth has four life stages: egg, larvae, pupae, and adult. During its larvae period, the larvae will undergo 8 to 10 molting stages, lasting from 28 days to 6 months before pupation (Ellis et al., 2013). Its feeding is more voracious in the earlier larval stages than in the latter ones. The larvae spin silk at all stages, but during the last larval stage, a silk cocoon is formed prior to their pupation (Jorjao et al., 2018). The pupal stage lasts between 1 to 9 weeks, before emerging as a moth (Figure 7; Kwadha et al., 2017).

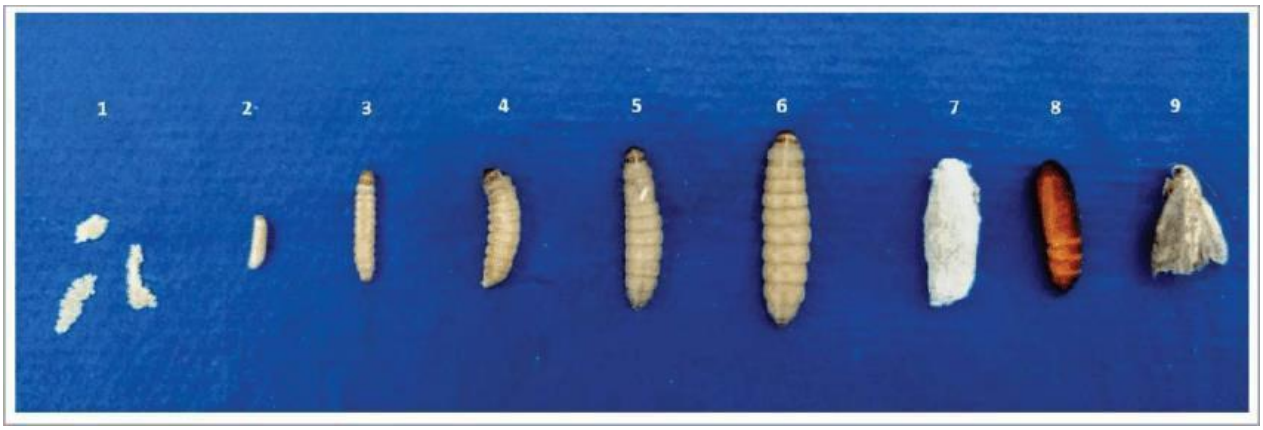

Figure 7. Developmental stages of *Galleria mellonella*. **(1)** Eggs. **(2)** 10-day-old larvae. **(3)** 20-day-old larvae. **(4)** 25-day-old larvae. **(5)** 35-day-old larvae. **(6)** approximately 40-day-old larvae (last larval stage. **(7)** Pre-pupae. **(8)** Pupae. **(9)** Adult moth. Image from Jorjao et al (2018).

Larvae are inexpensive, require no feeding during their last larval stage, and do not need special lab equipment for their maintenance. They can thrive at temperatures between 25 to 37°C, making them suitable to test microorganism behavior at mammalian temperature (Desalermos et al., 2012). Additionally, they have an innate immune system that models the mammalian immune system (Wittwer et al., 1999; Browne et al., 2013; Pereira et al., 2018).

Galleria mellonella larvae have been used as a model organism in insect pathology for over a century. Recently, they have been considered an infection model to replace small mammals (Pereira et al., 2018). In particular, they have served as model systems to study various human bacterial pathogens, including *Streptococcus pneumoniae*, *Enterococcus faecalis*, *Staphylococcus aureus*, *Listeria monocytogenes*, and *Escherichia coli* (Joyce and Gahan, 2010; Desbois and Coote, 2011; Loh et al., 2013; La Rosa et al., 2012; Williamson et al., 2014). Several fungal pathogens, such as *Candida albicans*, *Aspergillus fumigatus*, *Histoplasma capsulatum*, *Paracoccidioides brasiliensis*, *P. lutzii*, *Fusarium* species, and other *Cryptococcus* species, have also considered this insect for research (Coleman et al., 2011; Slater et al., 2011; Thomaz et al., 2013; Firacative et al., 2014; Bouklas et al., 2015; Scorzoni et al., 2015; Champion et al., 2016. Even viruses have been

investigated using *G. mellonella* larvae, such as the Tipula iridescent virus (TIV), Nodamura virus, and bovine herpes simplex virus-1 (BHSV-1) (Jafri and Chaudhry, 1971; Garzon et al., 1978; Büyükgüzel et al., 2007; Pereira et al., 2018). This model system has also proved effective for novel antimicrobial discovery (Andrea et al., 2019).

Larvae of *G. mellonella* have been used previously to assess the virulence of *Photorhabdus* and *Xenorhabdus* Pir toxins (Waterfield et al., 2005, Blackburn et al., 2006, Yang et al., 2017). With respect to research related to *Vibrio parahaemolyticus*, Wagley et al. (2019) proved *G. mellonella* to be excellent models. The researchers used last-instar larvae to assess non-toxigenic and toxigenic clinical strains of *Vibrio parahaemolyticus*, demonstrating the larvae were susceptible to all strains (Wagley et al., 2019).

Based on this background information, the overarching goal was to explore the insecticidal activity of *V. parahaemolyticus* Pir-like toxins using *G. mellonella* as the model organism.

CHAPTER 2: ASSESSING THE INSECTICIDAL VIRULENCE OF *VIBRIO PARAHAEMOLYTICUS* PIR-LIKE TOXINS

RESEARCH OBJECTIVES

In this study, we assessed *Vibrio parahaemolyticus* Pir-like toxins for their insecticidal activity considering *Galleria mellonella* last instar larvae as the model system. Specific goals of this study were:

Objective 1. To assess the insecticidal virulence of recombinant Pra and Prb binary toxin produced by *Vibrio parahaemolyticus* using *Galleria mellonella* larvae as the model host considering two different portals of entry, two dosages, and three experimental temperatures.

Hypothesis: The most effective portal of entry for these toxins will be the anal route, as these toxins affect the digestive route in its natural shrimp host, and the higher dosage will kill. The temperature that will result in the most killing is 28°C because in shrimp, this bacterium is more active when the waters are warm and therefore tends to cause AHPND in the summertime.

Objective 2. To evaluate and compare the insecticidal efficacy of recombinant Pra and Prb vs *Vibrio parahaemolyticus* toxins isolated from overnight culture.

Hypothesis: Recombinant proteins are synthesized with its Pra and Prb components separate, but proteins isolated from *V. parahaemolyticus* (#13-028, Strain A3), which produces Pir-like toxins and causes AHPND in shrimp, have both toxin components present and bound. The hypothesis is that the isolated proteins from *V. parahaemolyticus,* strain 13-028/A3, cell culture will be more virulent than the recombinant proteins because the proteins are secreted directly from the bacteria already bound and will be able to immediately deliver toxicity. Both recombinant and isolated proteins will exhibit virulence when compared to the control, *V. parahaemolyticus* ATCC #17802, which is a non-Pir toxin producing strain.

Objective 3. To investigate tissue specificity of Pir-like toxins in *Galleria mellonella* host using histology.

Hypothesis: Pir-like toxins may target the insect midgut tissue, as with *Photorhabdus* PirAB toxins, and thus it is predicted the cells will show pathological signs and tissue damage. Histological damage may be proportional to the tested Pir-like toxin concentrations.

MATERIALS AND METHODS

1. Pir-like toxins considered in this study

Recombinant Pra^{vp} and Prb^{vp} proteins and cell culture supernatant from *Vibrio parahaemolyticus* causing AHPND (#13-028, Strain A3) were considered in this study. The cell culture extract from *Vibrio parahaemolyticus* ATCC #17802 (ATCC® Global Bioresource) was used as a control for the virulence bioassays. The recombinant Pra^{vp} (GenBank accession No. KM067908) and Prb^{vp} (GenBank accession No. KM067908) proteins were expressed using an *E. coli* (BL21-DE3) expression system and custom made by GenScript® (BacPower™ Guaranteed Bacterial Recombinant Protein Expression Service, GenScript® Bank, Piscataway, New Jersey, USA). The codons *pra* and *prb* genes were optimized before expressing in *E. coli* BL21-DE3 (Mai et al., 2020). Recombinant proteins were purified to homogeneity and used for the virulence bioassays.

2. Isolation and purification of 13-028/A3 and the ATCC #17802 toxins

2.1 *Vibrio parahaemolyticus* bacteria growth

The 13-028/A3 and the ATCC #17802 proteins were purified directly from bacterial strains obtained from Dr. A. Dhar's laboratory (School of Animal and Comparative Biomedical Sciences, University of Arizona, Tucson, AZ, USA). Bacterial cultures were suspended in 5 mL of sterile Tryptic Soy Broth (TSB) with 2% NaCl in a 125 mL flask and incubated at 30ºC at 150 rpm for 2 h. After 2 h, 50 mL of TSB with 2% NaCl broth was added to the bacterial broth. The culture was incubated at 30ºC shaking at 150 rpm for 2 h. The solution was then transferred to a 2000 mL flask where 450 mL of TSB with 2% NaCl was added. The culture was then incubated overnight at 30ºC at 150 rpm (Sirikharin et al., 2015).

2.2. Isolation of proteins from *V. parahaemolyticus*

After overnight incubation, the culture was dispensed into 50 mL Eppendorf® tubes and centrifuged at 10,000 rpm at 4ºC for 30 min. The supernatant was discarded. The pellet left was resuspended in 50 mL of fresh 1X Phosphate Buffered Saline (PBS) by vortexing. The suspension was dispensed into 1.7 mL Eppendorf® tubes and centrifuged at 10,000 rpm at 4ºC for 10 min. The supernatant was then discarded, leaving a pellet in the Eppendorf® tubes.

Each Eppendorf® tube containing the pellet was vortexed for 3 min. Then, the pellet was ground completely with an autoclaved plastic pestle (VWR, Kontes® Pellet Pestle®, Kimble Chase). The Eppendorf® tubes containing the ground pellets were centrifuged at 8000 rpm at 4ºC for 10 min. The supernatant was filtered using a syringe fitted with a 0.2 µm filter (Acrodisc® 25mm Syringe Filter with 0.2 µm HT Tuffryn® membrane).

To confirm the isolation and purification of Pir-like proteins, 100 µL of purified solution of either 13-028/A3 or ATCC #17802 was pipetted onto a Tryptic Soy Agar (TSA) with 2% NaCl plate. The remainder of the purified protein solution was stored at -20ºC or in liquid nitrogen. Plates were incubated at 29°C overnight. The plates were checked the next day for bacterial colony growth or debris contamination. No bacteria colonies appeared, indicating that the purified proteins were free of bacterial contamination.

2.3 Bradford assay for isolated protein quantification

A Bradford Assay (Bio-Rad) was performed to determine the protein quantification of the purified bacterial proteins. The Bradford BSA standard protein was prepared by reconstituting the lyophilized Bovine Serum Albumin (BSA) with 20 mL of deionized water. The Bradford BSA

standard protein (10^0) was serially diluted in 1X PBS to yield dilutions of 10^{-1}, 10^{-2}, 10^{-3}, and 10^{-4}.

An inoculum of 10 µL of the standard and diluted Bradford BSA standard protein were added in their respective wells of a 96-well microplate and the wells were labelled accordingly. Ten µL of 13-028/A3 and ATCC #17802 proteins were also added to their respective wells and labelled accordingly. An amount of 200 µL of Coomassie Brilliant Blue G-250 dye was added to each well containing protein. The plate was incubated for 5 min. at room temperature (Figure 8). The absorbance was read at 595 nm using the iMark™ Microplate Reader (Bio-Rad) and Microplate Manager® Software.

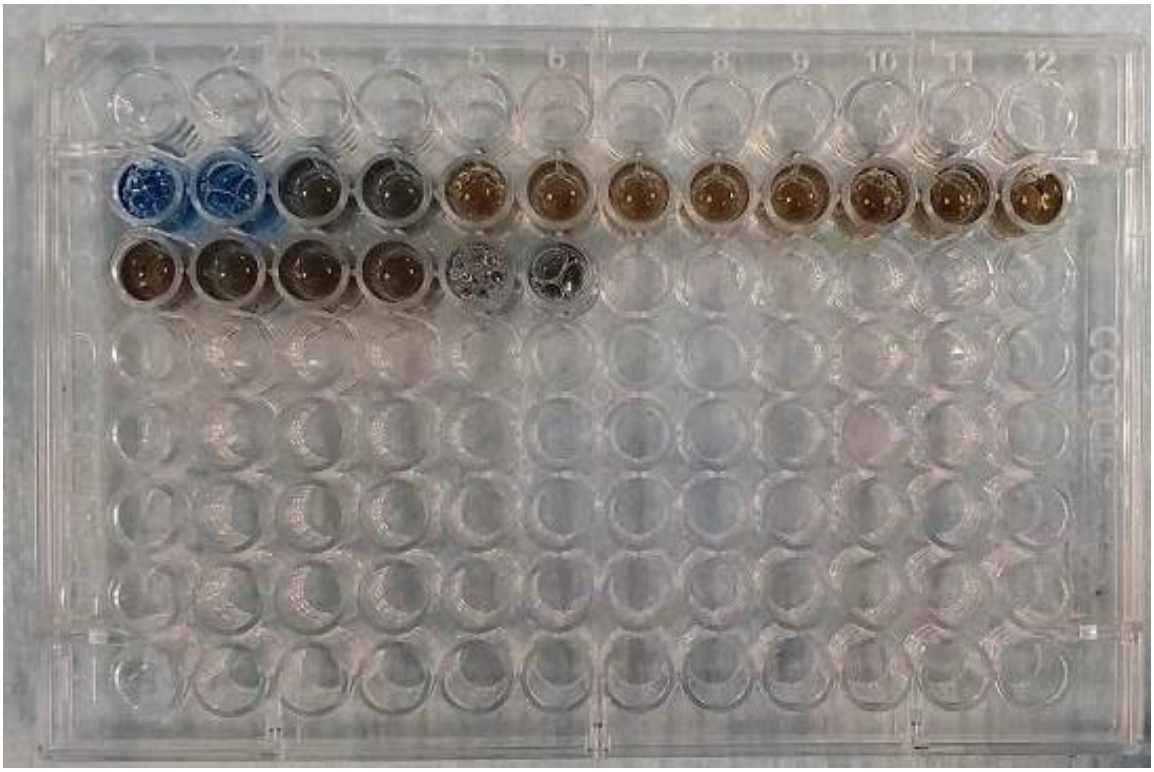

Figure 8. Bradford assay to determine the total protein quantification of protein in the purified solution. B1 - B2: 10^0 Bradford Reagent, B3 - B4: 10^{-1} Bradford Reagent, B5 - B6: 10^{-2} Bradford Reagent, B7 - B8: 10^{-3} Bradford Reagent, B9 - B10: 10^{-4} Bradford Reagent, B11 - B12: 1X PBS. C1 - C4: 13-028/A3 Purified Solution. C5 - C6: ATCC #17802 Purified Solution.

2.4 Identification and confirmation of Pra and Prb binary toxin in purified proteins with SDS-PAGE and Western Blot

An SDS-PAGE and a Western Blot assay were run to confirm the presence or absence of purified Pir-like toxins from the respective bacterial strains, 24 hr after purification. Protocols for running the SDS-PAGE and Western Blot assay were adapted from Xiao et al. (2017) and Victorio-De Los Santos et al. (2020). To prepare the samples for gel electrophoresis, 12 µL of 4x Laemmli sample buffer was added to 34 µL of purified sample in a 1.7 Eppendorf® tube on the day of the protein isolation. The tubes were incubated at 95ºC for 10 min. and stored in the -20°C freezer until the day of the SDS-PAGE and Western Blot were run.

The gels used were BioRad Mini-Protean® TGX™ Precast Gels. A 250 kDa ladder (BioRad Precision Plus Protein™ Dual Color Standard) was loaded. Each subsequent well was loaded with 5 to 10 µL of pre-incubated protein, followed by 4x Laemmli sample buffer. The loaded samples were standardized to the Bradford Reagent Concentration, so each well had approximately 10 µg of protein. The lower gel tank was half-filled with 1X SDS-PAGE Running Buffer (1X Tris/Glycine/SDS Buffer), and the upper gel tank was filled to the top with 1X SDS-PAGE Running Buffer. Both the SDS-PAGE and the Western Blot were run at 100V on the BioRad PowerPac™ for 2 h or until the samples reached the bottom of the gels (Figure 9).

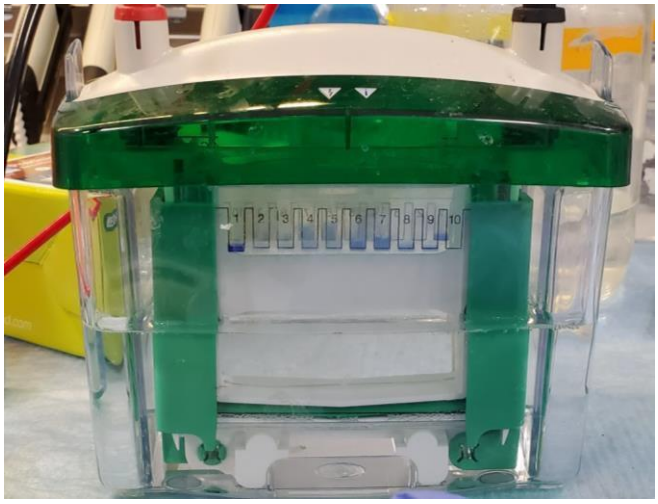

Figure 9. Electrophoresis setup for SDS-PAGE and Western Blot.

The SDS-PAGE was transferred to a plastic container. The gel was covered with Instant Blue to stain. The plastic container was then covered with cling film and moved to a rotator shaker overnight at 4ºC.

The Western Blot gel was moved to a transfer sandwich. The transfer sandwich was created following the Bio-Rad Electrophoresis and Blotting guide (Appendix B). The apparatus was then closed and moved to the tank. The tank was then filled with 1X Tris/Glycine Buffer until the sandwich was covered.

Parameters for running the Western Blot were: 70 mA ($1cm^2$ of filter paper = 1mA) for 120 min. After, the polyvinylidene difluoride (PVDF) membrane was transferred to a plastic container and 40 mL of 5% BSA Blocking Solution was added. The 5% BSA Blocking Solution was made with 2 g BSA and 40 mL of 1X Tris-Buffered Saline, 0.1% Tween® 20 Detergent (TBST). The solution was vortexed until mixed. The Western Blot was let to shake at room temperature for 2 h. After 2 h, a new batch of 40 mL of 5% BSA Blocking Solution was mixed. This time, 8 µL of recombinant Pra antibody and 8 µL of recombinant Prb antibody was added to

the blocking solution. The old BSA solution was replaced with the new 5% BSA Blocking Solution containing the recombinant antibodies. The Western Blot container was then covered with cling film and moved to a rotator shaker in the 4ºC fridge for 24 h.

After 24 h, both gels were washed with deionized water and rinsed in a rotator shaker for 1 h. A DryEase® Mini-Gel Dryer System and Gel-Dry™ Drying Solution were used to dry and preserve the finished SDS-PAGE.

The Western Blot membrane was rinsed three times with 1X TBST for 5 min. per rinse. After, 40 µL of 5% TSA was added in 1X TBST with 8 µL of Anti-Rabbit IgG Serum antibody and vortexed. The solution was added to the gel and left to shake on the rotator shaker for 1 h. The membrane was again rinsed three times with 1X TBST for 5 min. per rinse. After the last rinse, 200 µL of NBT (nitro-blue tetrazolium chloride)/BCIP (5-bromo-4-chloro-3'-indolyphosphate p-toluidine salt) was added. After 2 min., the membrane was rinsed with deionized water and dried.

3. Determining the insecticidal activity of Pra and Prb binary toxins produced by *Vibrio parahaemolyticus*

3.1. Insect source and parameters tested

Last-instar larvae of the greater wax moth *Galleria mellonella* (Lepidoptera: Pyralidae) used for these experiments were obtained from Timberline Fisheries (Marion Co., IL). Larvae weighing between 0.2 to 0.3 g were selected for these experiments.

Only the recombinant Pir-like toxins were considered in these experiments. Two different portals of entries were considered: the spiracles and the anus (Figure 10). The spiracles route delivered the toxins through the tracheas to the hemolymph and insect body cavity, whereas the anal route (aka reverse gavage) facilitated direct exposure to the insect gut and the digestive route.

Three different temperatures were tested: 22, 25, and 28°C. Two toxin concentrations were assessed: 0.1 and 0.5 µg (See section 3.2 below).

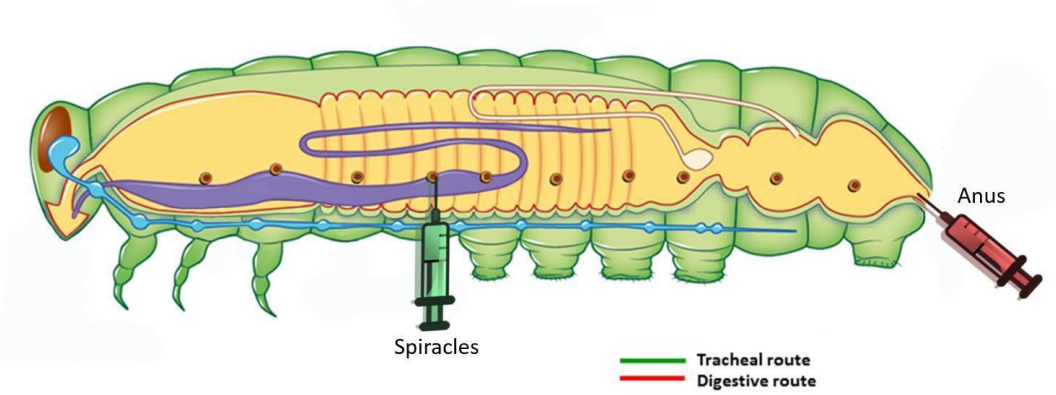

Figure 10. Diagram of injection routes into the *Galleria* mellonella larvae spiracles and anus (modified from Castagnola et al., 2016).

3.2. Dilution of recombinant Pir-like toxins and injection protocol

As mentioned above, this experiment only considered recombinant Pra and Prb toxins produced using a bacterial expression system (GenScript®). The Pra and Prb were stored in the -80ºC freezer or in liquid nitrogen until the day of experiments when they were retrieved and kept on ice to slow thawing.

Calculations for the two inocula tested (0.1 µg and 0.5 µg) are detailed in Appendix C. The two toxin complements Pra and Prb were combined 1:1 (Appendix C). Each protein suspension was prepared 30 min. apart and left on ice for 2 h to allow their individual Pra and Prb components to bind together. The tubes were then vortexed for 20 sec. and allowed to acclimate to room temperature for 5 min. prior to their injection into the larvae. Tubes were vortexed for 60 sec. immediately before being drawn into a syringe for injection.

Each insect larva was injected with a 10 µL volume containing the diluted toxins using a Syringe Microburet (No. SB2, Micro-Metric Instrument Co.) and disposable syringe (1 mL syringe

BD Luer-Lok™ Tip) with a 27-gauge needle (BD PrecisionGlide™ Needle, 27G x 1 ¼) (Figure 11; Zhang et al., 2014). Control treatments consisted of insects injected with 10 µL of 1X PBS (Wu and Yi, 2016). Prior to their injection, larvae were placed in a mesh strainer and sprayed with 70% ethanol. They were then placed on aluminum foil laid on top of an ice bucket to immobilize them before their injection.

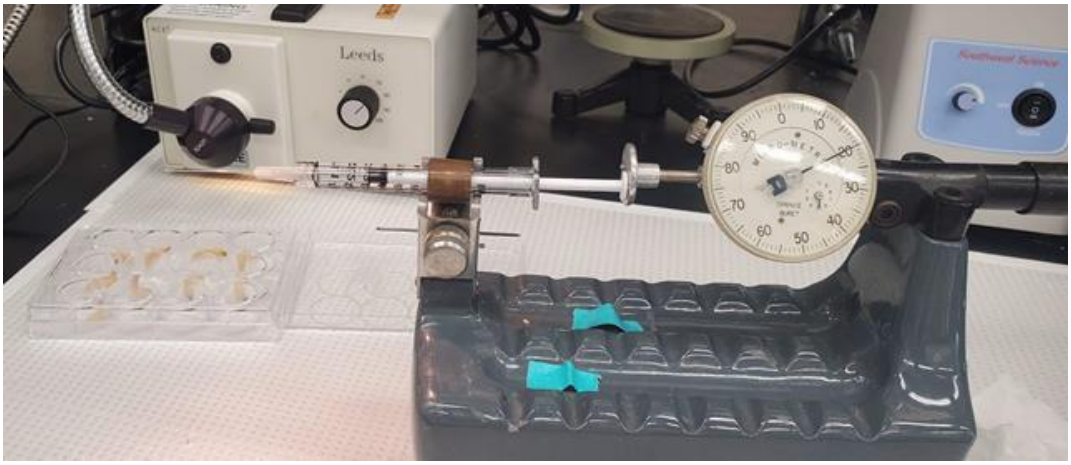

Figure 11. Microinjector and Injection setup.

3.3 Experimental design

The experimental arena was a 12-well plate (Falcon® 12-well Clear Multiwell Plate, Ref. 353225), where one *G. mellonella* was placed into each well. After larvae were injected and placed in their respective well, the plates were kept in incubators at each of the tested temperatures. Observations were made every 24 h to assess their mortality. Figure 12 illustrates the experimental design and shows the appearance of larvae on day 0, the first day of injections. At day 7, larvae with dark color due to melanization and that did not react to stimulus via gentle prodding with forceps were considered dead. Larvae that pupated during the experiments were scored alive since they responded to stimulus via gentle prodding and were continuing their metamorphosis (Figure

13). Experiments were repeated six times in the anus route of injection and three times in the spiracles route of injection.

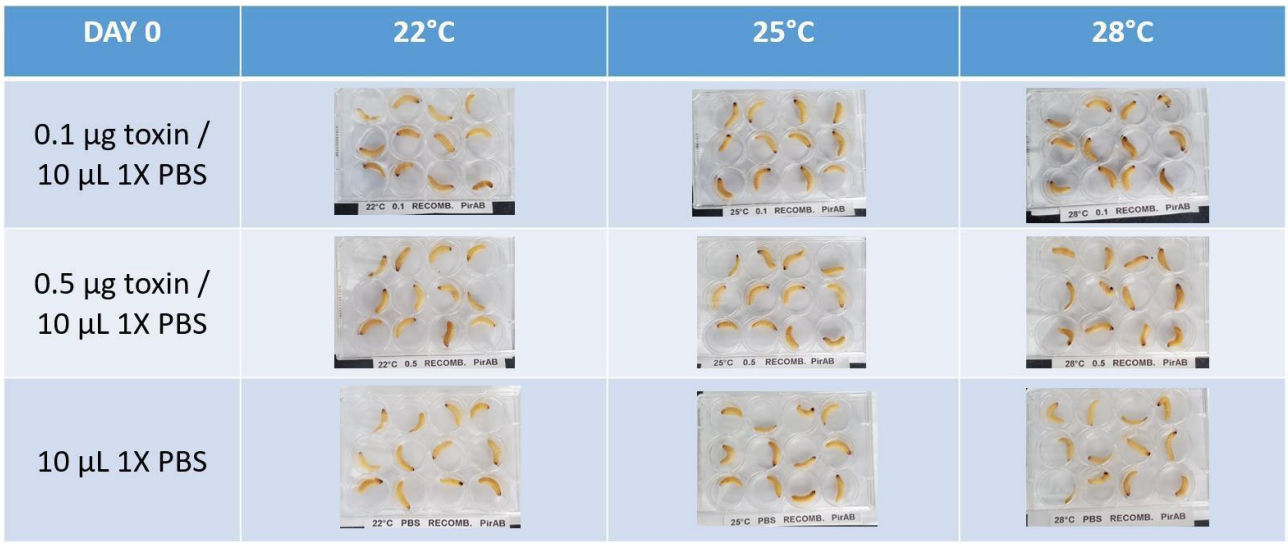

Figure 12. Schematic representation of the portal of entry experimental design. This design illustrates the anal route of injection in all temperatures on day 0.

Healthy Dead Pupae

Figure 13. *G. mellonella* larvae. **(Left)** Healthy, alive larvae. **(Middle)** Dead larvae. **(Right)** Pupa. The pupae cocoon colors range in color from dark brown to light yellow.

4. Comparing the insecticidal efficacy of recombinant Pra and Prb vs *Vibrio parahaemolyticus* toxins isolated from overnight culture

4.1. Experiment parameters

These experiments were conducted to compare the activity of the recombinant protein, which was synthesized with its Pra and Prb components separate, with the purified cell culture supernatant from *V. parahaemolyticus* causing AHPND (#130-28, Strain A3) where both toxin components were already present. As a negative control, total secretary protein isolated from a *V. parahaemolyticus* strain, ATCC #17802, that does not produce Pir-like toxins was included. Control treatments also consisted of insects injected with 10 µL of 1X PBS. These experiments were carried out at 25°C and only the anal route of injection based on results obtained from the virulence experiments. *Galleria mellonella* selection, larvae injection, and larvae mortality score was the same as described in Section 3.1, 3.2, and 3.3, respectively.

4.2 Experimental design

The experimental setup was similar to that used for the virulence experiments. Figure 14 shows the experimental design comparing the different protein sources on Day 0. Experiments were repeated three times for each protein source and dosage. The dead and alive scoring was the same as in the previous experiments (Section 3.3).

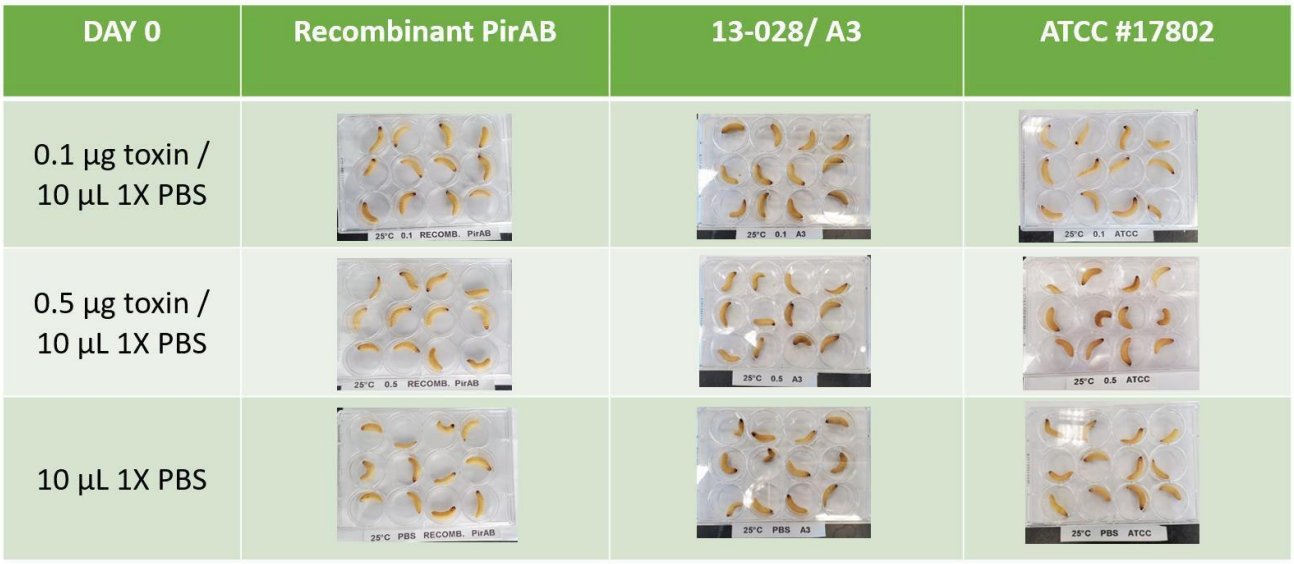

Figure 14. Schematic representation of the protein source experimental design. This design illustrates the three protein sources and dosages in 25°C on Day 0.

4.3. Dilution of 13-028/A3 and ATCC #17802 proteins

Two dosages were considered: 0.1 µg and 0.5 µg. The recombinant Pir-like toxins were prepared as described previously in Section 3.2. Protein dosages for 13-028/A3 and the ATCC #17802 were prepared based on the concentrations obtained from the Bradford Reagent Concentration, as performed above in Section 2.3. See Appendix D for calculation details. The protein suspensions and dosages were prepared 30 min. apart. The tubes were then vortexed for 20 sec. and allowed to acclimate to room temperature for 5 min. prior to their injection into the larvae. Tubes were vortexed for 60 sec. immediately before being drawn into a syringe for injection.

5. Statistical analysis

Analysis of data considered a chi-square test to test for differences of total mortality among the variables. Variables included were injection site, temperature, dosage, and protein

source. Descriptive statistics were computed using the PROC FREQ command in SAS University Edition software (Cary, NC: SAS Institute Inc. Accessed 6-10-20). A cox regression was also chosen to run descriptive statistics because it investigates the effects of several simultaneous variables each against the other. The statistical package used was IBM SPSS 26 (IBM Corp., 2019).

Abbott's formula was used to correct for mortality in the control group when higher than 5% (Abbott, 1925; WHO, 2016).

6. Histological Observations

6.1. Fixation protocols

Moribund and healthy *G. mellonella* larvae were processed for histological observations. Larvae were placed in a freezer at -20°C for 2 to 3 min. to cold shock them. Larvae were then processed for further fixation in different ways. Some larvae were injected in the back, sides, and stomach with approximately 0.15 mL of Carnoy's fixative. Smaller larvae did not need the full 0.15 mL of Carnoy's fixative, so they were injected until the body was rigid. They were then transferred to a 1.7 mL sterilized microcentrifuge tube with Carnoy's fixative. Other larvae were not injected with additional Carnoy's fixative and following cold-shock, were immediately moved into a 1.7 mL sterilized microcentrifuge tube with Carnoy's fixative or 10% formalin.

Larvae fixed with either Carnoy's fixative or 10% formalin were kept at varying temperatures and fixation times. Individual larvae were either maintained at either room temperature in the fume hood or placed in the 4°C fridge. Only variants of larvae fixed with Carnoy's fixative were placed in the 4°C fridge and of those, some were wrapped with aluminum

foil to avoid degradation of the fixative by light (Perdoni et al., 2014). Fixation time tested was 2, 3, 4, 24, and 48 h.

After fixation, larvae were gently removed from the fixative and rinsed twice with 70% ethanol. Finally, individual larvae were placed in a new 1.5 mL microcentrifuge tube filled with sterile 70% ethanol (Becnel, 2012). The samples were stored at room temperature in the fume hood until the time they were processed.

6.2. Histological sectioning of the specimens

Fixed *G. mellonella* larvae were embedded in paraffin following standard procedures described by Lightner (1996). Tissues were embedded in paraffin using the Sakura Tissue Tek TEC5 embedding console system and processed with the Sakura Tissue TEK VIP E300 tissue processor. After paraffin embedding and processing, 4 µm-thick sections were obtained with a Microm^{TM} ultramicrotome (Microm, HM355s). Tissue sections were stained with hematoxylin and eosin (H&E) for light microscopy following procedures described by Lightner (1996) and Dhar et al. (2019). Figure 15 summarizes the histology workflow.

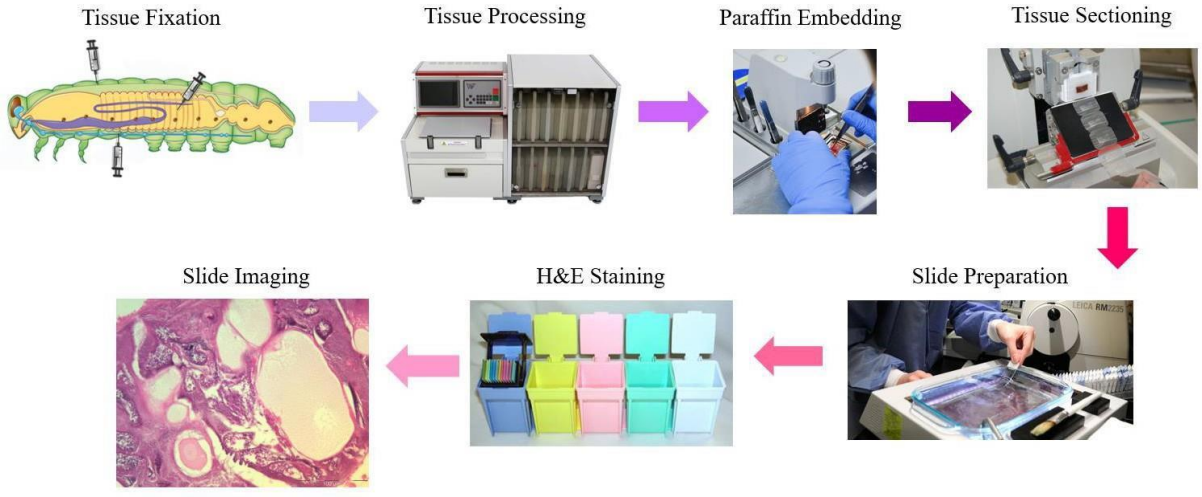

Figure 15. Histology workflow from tissue fixation to slide preparation for histological observations.

RESULTS

1. Confirmation of 13-028/A3 and the ATCC #17802 toxin identity

The concentrations of proteins isolated from the overnight culture supernatant of *V. parahaemolyticus* (#13-028, Strain A3) and *V. parahaemolyticus* ATCC #17802 Strain were 0.5 µg/µL and 1.0 µg/µL, respectively. SDS-PAGE and Western Blot further confirmed the identity of the Pra and Prb toxin components. Lane 1 and Lane 2 show bands for Pra (white arrow at 15 kDa) and Prb (black arrow at 50 kDa) from 13-028/A3. Lanes 3 and 4 show no bands for ATCC # 17802 purified proteins, confirming the absence of Pir toxins in this strain. Lane 5 is a positive control of purified and confirmed 13-028/A3 Pra (white arrow) and Prb (black arrow) proteins (Figure 16A).

The Western Blot further confirmed the presence of Pra and Prb. Lane 1 and Lane 2 represent strain 13-028/A3 and show present Pra and Prb; whereas, Lane 3 and 4 for ATCC #17802 purified proteins show no bands, confirming that the ATCC #17802 does not have Pir-liketoxins. Lane 5 is a positive control of previously purified 13-028/A3 showing presence of Pra and Prb proteins (Figure 16B).

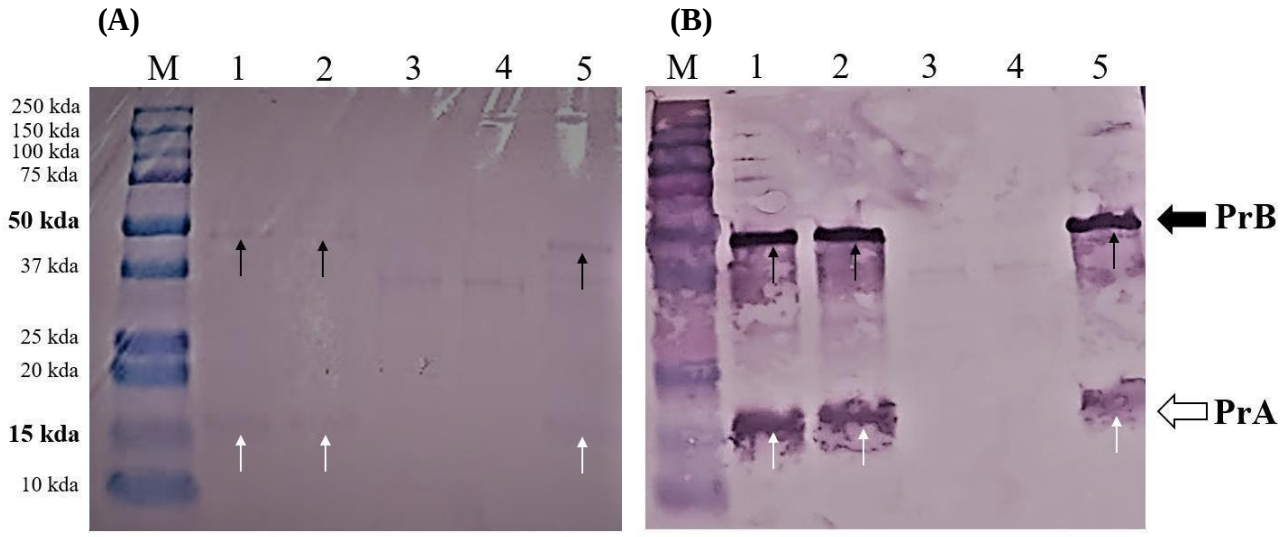

Figure 16. **(A)** SDS-PAGE, **(B)** Western Blot, confirm presence of purified *Vibrio* PirAB-like toxins. Black arrows: Prb bands at 50 kDa. White arrows: the Pra bands at 15 kDa.

2. Determining the insecticidal activity of Pra and Prb binary toxins produced by *Vibrio parahaemolyticus*

Our results showed that overall insect mortality was generally low, not exceeding 14.3% when the toxins were delivered via anal route at 0.1 µg/larvae, and the larvae were incubated at 22°C following injection (Table 2). For this route and when comparing all temperatures tested, it was clear that at 22°C, the virulence of *Vp* Pir-like toxins was the highest; however, there was no significant effect of the temperature on larvae mortality (Figure 17; p-value: 0.77, X^2: 0.53, df: 2). Interestingly, the recombinant toxins showed a higher virulence at the lower inoculum, 0.1 µg, for all tested temperatures (Figure 18). However, when dosage mortality was compared to the control, differences were not considered significant (p-value: 0.08, df: 2, X^2: 5.107).

Under the spiracles portal of entry, Pir toxins showed very low virulence as reflected by none or very low insect mortality. Only at 25°C, a modest insect mortality (5.6%) was achieved for the high dose, 0.5 µg (p-value: 0.36, X^2: 2.02, df: 2). No treatment insect mortality was observed at 22 and 28°C, although there was 1.9% insect mortality in the control at 22°C (p-value: 0.36, X^2: 2.02, df: 2) (Table 3).

When comparing results for the two portals of entry, the digestive route showed the highest mortality and that there was a significant effect between anus and spiracles, with the anal route of injection causing significantly higher mortality in *G. mellonella* larvae (p-value: 0.00; df: 1) (Figure 19). These differences are shown as a probability of death at the time that the insects died.

Table 2. Percent mortality (Abbott corrected) for anus portal of entry and raw percent mortality for spiracles portal of entry

Temperature (°C)	Dosage (µg)	Anus Mortality (%)	Spiracles Mortality (%)
22	0.1	14.3%	0.0%
	0.5	3.2%	0.0%
	Control	0.0%	1.9%
25	0.1	6.6%	0.0%
	0.5	3.2%	5.6%
	Control	0.0%	0.0%
28	0.1	8.3%	0.0%
	0.5	0.0%	0.0%
	Control	0.0%	0.0%

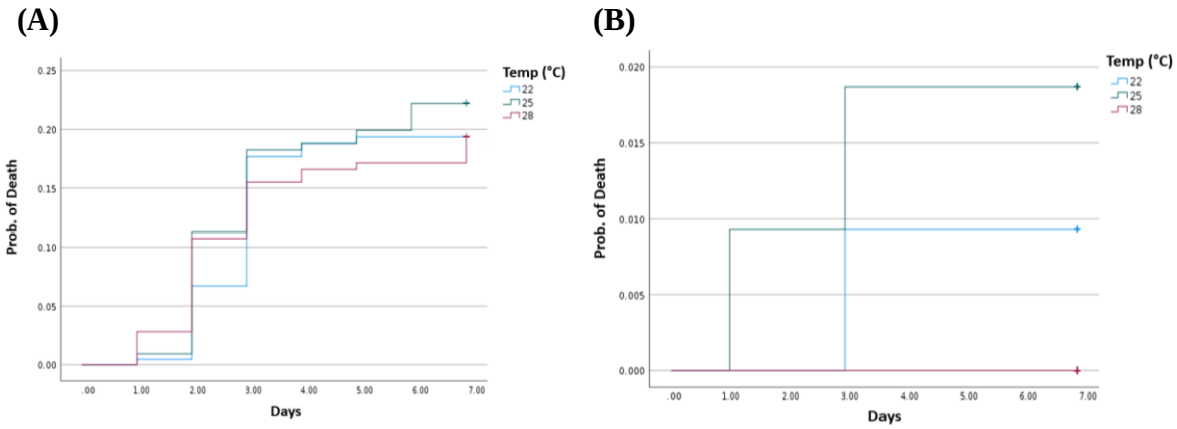

Figure 17. Effect of temperature on probability of insect death over time (days) for **(A)** anus portal of entry (p-value: 0.77, X^2: 0.53, df: 2) and **(B)** spiracles portal of entry (p-value: 0.36, X^2: 2.02, df: 2). Raw data, not corrected, was used for this analysis. Neither portal of entry had a significant temperature effect on insect mortality.

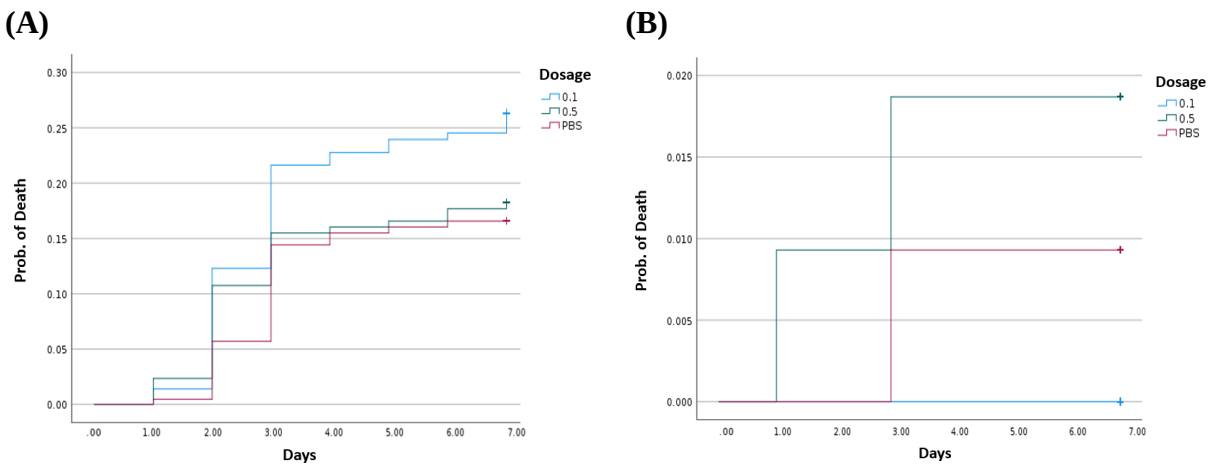

Figure 18. Effect of dosage on probability of insect death over time (days) for **(A)** anus portal of entry (p-value: 0.08, df: 2, X^2: 5.107) and **(B)** spiracles portal of entry **(**(p-value: 0.36, X^2: 2.02, df: 2). Raw data, not corrected, was used for this analysis. Neither portal of entry had a significant dosage effect on insect mortality.

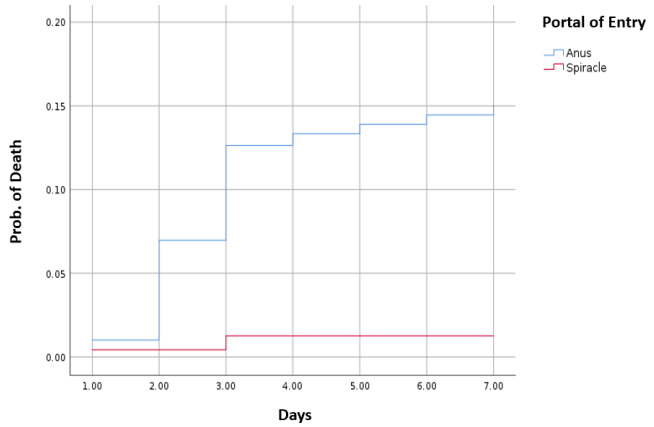

Figure 19. Effect of dosage on probability of insect death over time (days) for both anus and spiracles portal of entries (p-value: 0.00; df: 1). Raw data, not corrected, was used for this analysis. The anal portal of entry caused significantly higher mortality in larvae than the spiracles portal of entry.

Since mortality was assessed every 24 h and for a 7-day period, time to death was reported for the anal portal of entry comparing the two doses tested. Since temperature did not have a significant effect on toxin activity, mortality for all tested temperatures was pooled together. Figure 20 displays the highest mortality in the anal portal of entry was achieved on day 2. The highest

insect mortality was 20% at the 0.1 µg dose, and an 8% insect mortality was observed with the 0.5 µg dose. Day 3 observed an 8% insect mortality for the 0.1 µg dose. Thereafter, no mortality was observed.

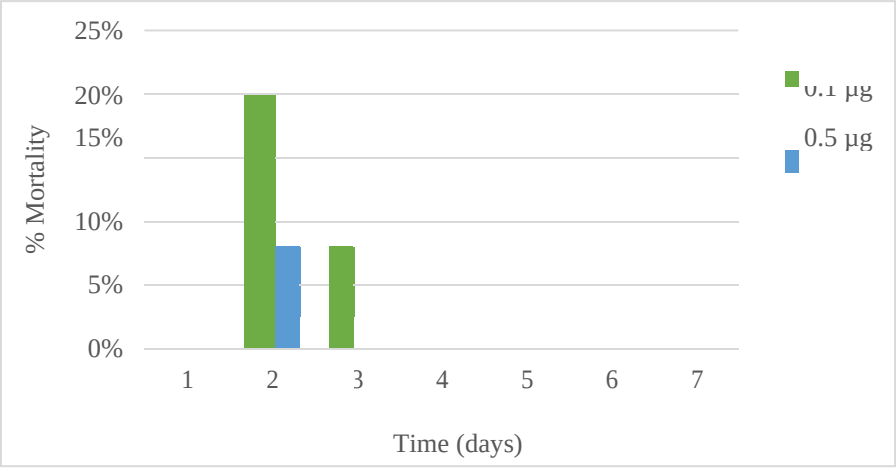

Figure 20. Corrected percent mortality of *G. mellonella* larvae that died per day for the anal portal of entry. Percent mortalities were corrected per day based on the Abbott's formula.

3. Comparing the insecticidal efficacy of recombinant Pra and Prb vs *Vibrio parahaemolyticus* toxin isolated from overnight culture

Results from these experiments showed that overall insect mortality was generally low, not exceeding 21.5% for the recombinant PirAB source at the 0.1 µg dose (Table 4). When comparing all protein sources tested, it was clear that for the 0.1 µg dose, the virulence of recombinant Pir-like toxins was higher (p-value: 0.001, df: 2) (Figure 21). These results are similar to those observed in the previous experiments. No mortality was observed in the larvae treated with the 13-028/A3 protein (p-value: 0.428, df: 1). Surprisingly, mortality was observed in the control strain ATCC #17802, which is a strain that does not produce Pir-like toxins, for the two doses tested (Table 4). However, when dosage mortalities were compared to the 1X PBS

negative control, mortality for either dosage (0.1 µg: p-value: 0.10, df: 1; 0.5 µg: p-value: 0.41, df: 1) was not significant (Figure 22).

Table 3. Percent mortality (Abbott corrected) for mortality among protein source

Protein Source	Dosage (µg)	Mortality (%)
Recombinant PirAB	0.1	21.5
	0.5	14.3
13-028/A3	0.1	0.0
	0.5	0.0
ATCC #17802 (Control)	0.1	21.1
	0.5	3.1

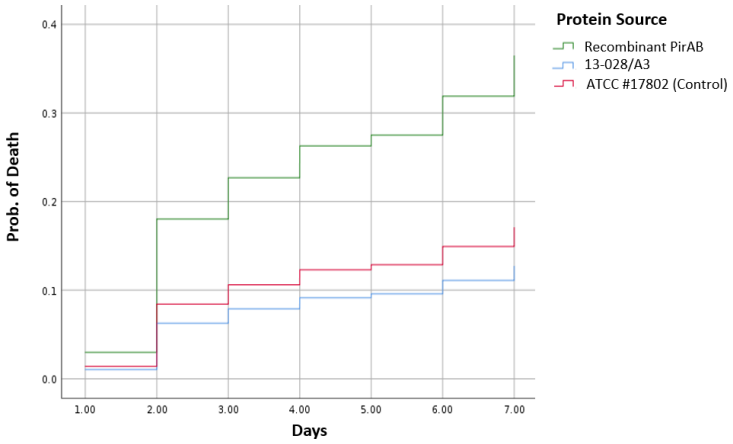

Figure 21. Effect of protein source on the probability of insect death over time (days). Raw data, not corrected, was used for this analysis. The recombinant PirAB source had the highest amount of killing (p-value: 0.001, df: 2), followed by the ATCC #17802 purified proteins, which do not contain Pir-like toxins, and the 13-028/A3 purified proteins, which do contain Pir-like toxins.

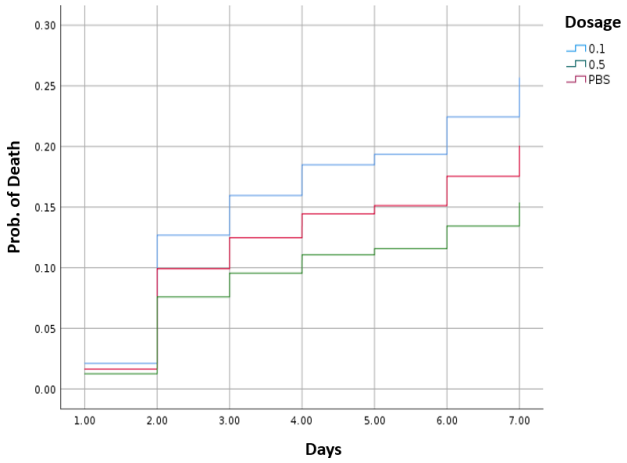

Figure 22. Effect of dosage on the probability of insect death over time (days). Raw data, not corrected, was used for this analysis. With all protein sources compiled, neither dosage showed significance (0.1 µg: p-value: 0.10, df: 1; 0.5 µg: p-value: 0.41, df: 1).

Since larvae were observed every 24 h for mortality, larvae death times were analyzed. The highest larvae mortality occurred on day 2, day 4, and day 6 with approximately 15.0%, 14.0%, and 9.0% overall mortality, respectively, for the recombinant PirAB protein source (Figure 23). Day 1 and 3 resulted in low insect mortality at 3%. No insects died on day 5 or day 7. For the ATCC #17802 protein, the highest mortality occurred on day 3, with approximately 14.0% mortality. Similar mortalities occurred on day 1 and 2 at about 5% mortality, and day 4 and 6 at 3% larvae mortality (Figure 23). No insects died on days 5 and 7.

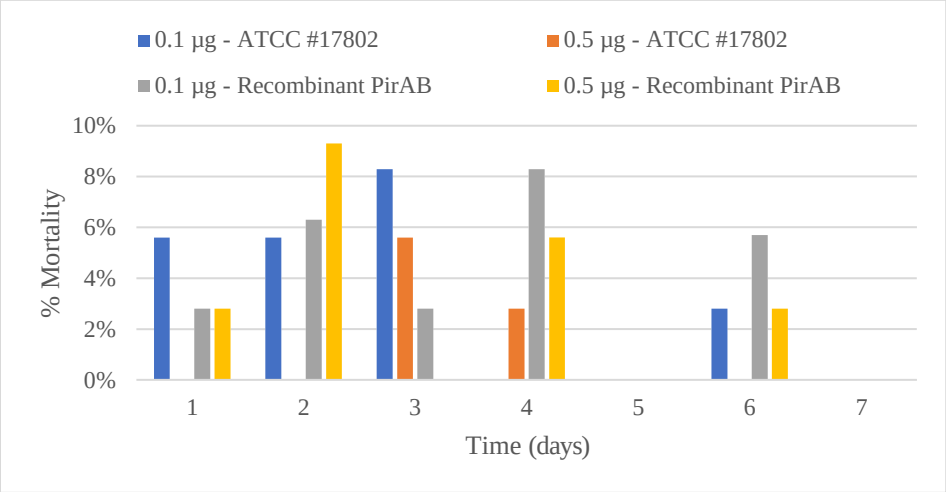

Figure 23. Corrected percent mortality of *G. mellonella* larvae that died per day in the protein source experiments for the ATCC #17802 control strain and the Recombinant PirAB treatment. Percent mortalities were corrected per day, using the Abbott's formula.

4. Histological Analysis

4.1. Fixation Procedures

Moribund and healthy *G. mellonella* larvae were processed for histological observations. Of the two different fixatives used, Carnoy's fixative worked more effectively than 10% formalin in preserving the integrity of the larvae tissues. Fixation of larvae with 0.15 mL of Carnoy's fixative through multiple injection sites (back, sides, and stomach) showed better results when compared with those larvae directly immersed in fixative.

As for the preservation of the samples, the larvae preserved in tubes wrapped with aluminum foil yielded better preserved larvae than those placed in unwrapped tubes. When comparing storage temperature, samples kept at 4°C fridge for 24 h yielded better results than those stored at room temperature for the same period of time. For each of these, those that yielded worse results were unable to be make tissue sections, as the tissues did not hold together and fell

apart when cut with the microtome. Larvae fixed with 10% formalin were also not suitable for microtome sectioning and were discarded.

Both 10% formalin and Carnoy's fixative have been used effectively in *Galleria* histology literature. One such study was performed by Card et al. (2016) where 10% formalin was used and the insects were let to fix for 7 days at room temperature. Becnel (2012) also explained that insects could effectively be fixed with Carnoy's fixative at room temperature for 24 to 48 h.

4.2 Midgut Histology

The midgut of healthy *G. mellonella* larvae showed the typical single layer epithelium with clear microvilli (Figure 24).

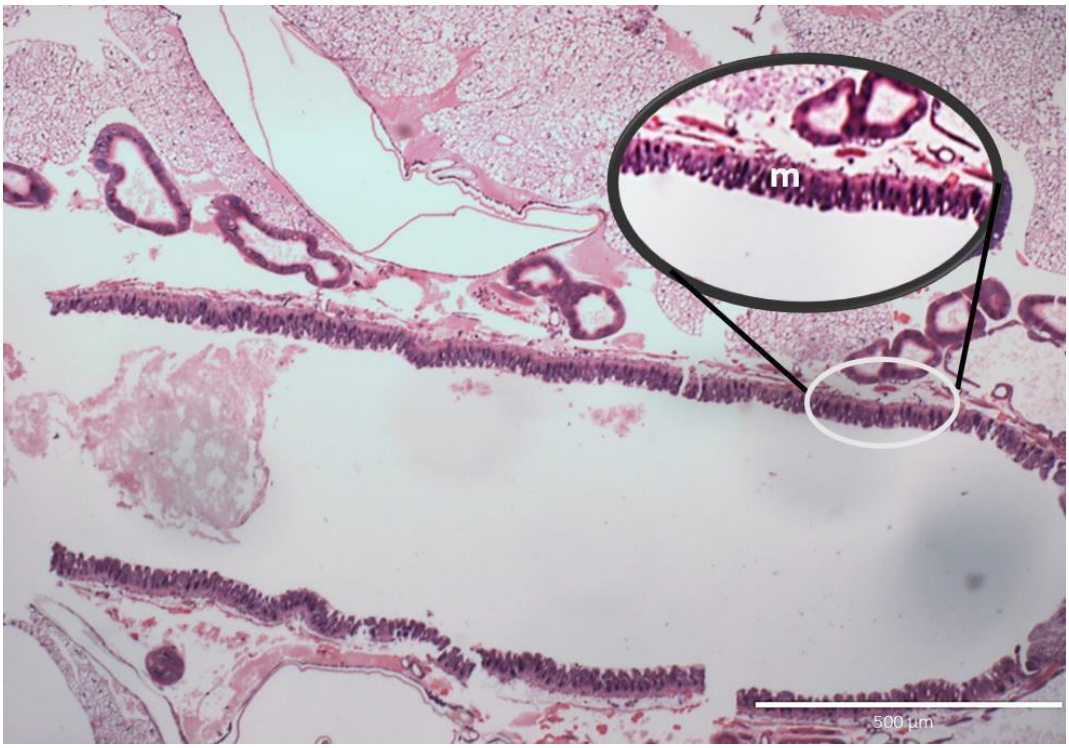

Figure 24. H&E longitudinal section of midgut of healthy *G. mellonella* larvae (100x). M: microvilli.

Contrarily, the epithelial cells of the midgut of larvae exposed to recombinant PirAB (0.1 µg) via the anus portal of entry show lack or shortening of microvilli and a potential swelling of the columnar cells (Figure 25). The columnar cells also appear compressed with clear spaces visualized within, which may be a result of a dilated endoplasmic reticulum or Golgi complex (Haschek et al., 2010).

Figure 25. H&E longitudinal section of midgut of *G. mellonella* larvae injected with 0.1 µg of recombinant Pir toxins (100x). CC: Columnar Cells. M: microvilli.

DISCUSSION

Vibrio parahaemolyticus is an important pathogen of shrimp and other aquatic animals with economic relevance to the food industry. This bacterium produces a variety of toxins, such as *tdh* (thermostable direct haemolysin) and *trh* (TDH related haemolysin) which are known to cause gastroenteritis in humans (Letchumanan et al., 2014). In 2015, novel proteins with toxic activity were found in connection with Acute Hepatopancreatic Necrosis Disease (AHPND) in shrimp (Hong et al., 2016; Li et al., 2017). AHPND targets the shrimp hepatopancreas and causes nearly 100% mortality within 20 to 30 days of first infection (Han et al., 2015; Lee et al., 2015). These toxins are similar to *Photorhabdus* insect related (Pir) toxins and are thus referred to as Pir-like.

These toxins have a binary structure, with two components: Pra and Prb. Both components are required to cause mortality in insects (Waterfield et al., 2005; Ahantarig et al., 2009). *Photorhabdus* Pir proteins, which are known to be insecticidal, are homologs of *Vibrio* Pir-like toxins, which cause rapid killing in shrimp. However, the insecticidal activity of *Vibrio* Pir-like toxins has not yet been assessed. Thus, in this study, we examined the effect of temperature, portal of entry, and toxin dose considering *G. mellonella* as a model system.

Overall, our results showed these toxins had very low insecticidal activity. When comparing portals of entry, the anus route seemed to favor the virulence of the toxins. *Vibrio* Pir-like toxins have been shown to have a direct effect on the digestive system (hepatopancreas) (Hong et al., 2016; Li et al., 2017). In this respect, our results showed that the anal route could be a more effective portal of entry in *G. mellonella* larvae as a direct route to target the midgut tissue. Based on the preliminary histological observations, it could be speculated that this is the case. The histology observations showed that the treated larvae exhibited none or shortened

microvilli, with a compression of the columnar cells. However, there were histological differences than the results shown in Blackburn et al. (2006) where there was damage to midgut epithelial cells and shedding and swelling of the apical gut membranes within *Plutella xylostella* larvae (Blackburn et al., 2006). With AHPND, Pir-like toxins cause the hepatopancreas tubule epithelial cells to detach from the basement membrane and get sloughed into the tubule lumen (Tran et al., 2013; Han et al., 2015). Therefore, since the histology observed in this study is different than the described above, it remains unknown the mechanism for the precise mode of action of the Pir-like toxins in insects.

When assessing the effect of temperature, a higher mortality was observed in 22°C in the digestive route assays. However, these differences were not significantly different from a statistical standpoint. With respect to dose effect, there was a trend for a higher mortality with the lower dose of 0.1 µg in the anus portal of entry experiments.

For the spiracles route of injection, the insect mortality was low or non-existent. Results from these experiments showed puzzling outcomes when assessing the effect of temperature and dose response. Here, the only treatment that showed larvae mortality was at 25°C with the 0.5 µg dose (5.6%). This is contrary to the anus portal of entry, which showed higher mortality (6.6%) at the 0.1 µg dosage at 25°C. All together these results suggest that portal of entry and, in particular via the digestive route, plays a role in the virulence of the toxins.

Furthermore, dependence on the biological activity of the toxin may also be dependent on temperature, at least when considering the digestive injection route. In this study, the highest mortality was achieved at 22°C. This is contrary to the shrimp host system because *Vibrio* species are more active in 28°C water so *Vibrio* outbreaks, and subsequently AHPND infections, in shrimp typically happen in the summer (Karunasagar et al., 1994).

With respect to the doses tested, concentrations were based on experiments performed by Wu and Yi (2016). The experiments performed were similar to this study in that the researchers injected purified recombinant *Photorhabdus luminescens* Pir toxins directly into the *G. mellonella* hemocoel. Dosages used in their experiments ranged from 90 ng (0.09 µg) to 240 ng (0.24 µg) injected in a total volume of 10 µL per larvae. As a negative control, the team injected 10 µL of 1X PBS (Wu and Yi, 2016).

In experiments involving the anal portal of entry, the 0.1 µg dose showed higher mortality than the 0.5 µg dose. One explanation for how the low-dose induced mortality may be attributed to an enzyme-substrate relationship as seen in the mode of action of the Bt Cry toxins (Schnepf et al., 1998). In the alkaline pH of the insect gut, Cry toxins are cleaved by proteases, which activate the toxins to bind to its target cells (Schnepf et al., 1998). In the shrimp system, there are biological reactions that seem to stimulate increased *Vibrio* Pir-like toxin release. These reactions include rho signaling pathway activation and likewise activate a GTPase, RhoA, and increased bile acid (Lim et al., 2014; Ng et al., 2018; Kumar et al., 2019).

There may also be untested factors, similar to the protease cleaving of Bt from its inactive form to its active form. The toxin stimulators that exist in shrimp may not exist in *G. mellonella* larvae, thereby only stimulating low activity by Pir-like toxins. Another possible explanation could be that a relationship could exist between the binding action of the toxin and the available receptor on the host cell. *G. mellonella* may not have the same cell receptors that the shrimp hepatopancreas does to facilitate PirAB-like toxin to cell infection.

Lastly, in another experiment, Machado et al. (2017) found that Dipel, a commercial Bt formulation, had low dose toxin effects when given to a non-target animal. The researchers tested concentrations of 0.001 to 1000 µL treatment dissolved per L of water on neonate and

adult *Daphnia magna* (Cladocera: Daphniidae). 100% mortality was observed between 1 to 10 µL treatment dissolved per L of water in both the neonate and the adult groups (Machado et al., 2017).

The two experiments conducted using recombinant PirAB showed varied mortalities with a similar trend. The first experiment comparing the portals of entry exhibited that recombinant PirAB had a total insect mortality of 29.2% at 0.1 µg and 6.5% at 0.5 µg through the anal portal of entry. The second experiment, which compared recombinant PirAB to the toxins isolated from the bacterial strains, resulted in recombinant PirAB causing an insect mortality of 21.5% at 0.1 µg and 14.3% mortality at 0.5 µg. These differences could be attributed to two different batches of recombinant PirAB proteins that were ordered and utilized in these experiments in regard to production and handling. However, they both show a similar trend of the lower dose having higher mortality than the higher dosage.

When comparing the effect of recombinant toxins to the 13-028/A3 cell filtrate, this study showed that recombinant PirAB proteins caused higher mortality (21.5% total mortality) than the cell filtrate proteins for the 0.1 µg dose. Similar results were observed for the 0.5 µg dose with a 14.3% total mortality for the recombinant PirAB protein and no mortality for the 13-028/A3 protein. However, low statistical values indicated that these mortality rates were not significantly different from the negative control (1X PBS) mortality rates.

The ATCC #17802, which does not produce Pir-like toxins, had a higher mortality rate than 13-028/A3, which does produce Pir-like toxins. This could be attributed to the fact that ATCC #17802 is a human-isolated *Vibrio* pathogen; whereas, the 13-028/A3 strain is a shrimp-isolated strain. *Galleria mellonella* has been shown to be an effective model system for studying human disease, since they can survive in temperatures up to 37°C, normal human body

temperature, and possess a similar innate immune response to that of mammals (Wittwer et al., 1999; Desalermos et al., 2012). *Galleria* larvae are also highly susceptible to clinical *Vibrio* infections, given their weak immune systems (Tsai et al., 2016; Pereira et al., 2018; Wagley et al., 2018). Therefore, while *Galleria* have been shown to be excellent models for human pathogens, they have not been investigated in terms of shrimp pathogens.

Overall, these data show that *Vibrio* Pir-like toxins may have a limited host range (Hao et al., 2019). In a recent study, Hao et al. (2019) tested the host range of the *Vibrio* Pir-like toxins in bloodworms (*Nereis succinea*), crabs (*Eriocheir sinensis*), European seabass (*Dicentrarchus labrax*), mosquitoes (*Aedes albopictus*), and shrimp (*Litopenaeus vannamei*). Their results showed only very low mortality in bloodworms (2%), when compared to shrimp where an 87% mortality was recorded (Hao et al., 2019).

Furthermore, research should also be directed at assessing the effect of *in vitro* association of Pra and Prb. In this study, 2 h were allotted to allow for protein binding based on Pir binding mechanisms researched by Lin et al. (2019). According to Lin et al. (2019), these toxins form an unstable complex and have low binding affinity; therefore, the 2 h in this study may have been too much or too little time to allow for binding. As other studies investigating recombinant Pir proteins do not incorporate binding time, future research should be directed towards this (Li et al., 2014; Wu and Yi, 2016).

Overall, the virulence of *Vibrio* Pir-like toxins in *Galleria mellonella* larvae was low, but there may still be potential for furthering investigation in relation to their insecticidal activity. Future studies should expand the host range targeting insects of different orders. Focus should also be placed in developing a dose response considering a lethal concentration.

Histological Challenges and Considerations

An unexpected challenge came with the fixation process of *G. mellonella* larvae with Carnoy's fixative. Although the Carnoy's fixative worked well for surface tissues, when the larvae were cut deeper in sagittal layers with the microtome to investigate organs, the tissues fell apart and tissue sections could not be made. A possibility for this could be because the larvae were embedded in paraffin following a procedure that is optimized for shrimp as described by Lightner (1996). Additionally, Becnel (2012) describes the appropriate dehydration series for dehydrating and embedding fatty insect larvae; however, the Sakura Tissue TEK VIP E300 tissue processor dehydration series used were optimized for shrimp, which contain more muscle than larvae and therefore require different dehydrations (Lightner, 1996).

Other studies used variable methods of fixation for histology with decisive results. Card et al. (2016) studied *G. mellonella* midgut histopathology in regard to *Salmonella enterica* Typhimurium affecting a bovine livestock population. At 24 h, infected larvae were chilled at 4°C for 2 hours prior to fixation and then fixed in formalin for 7 days at room temperature before processing and staining with H&E. The fixed and processed larvae specimens were then cut longitudinally, and the gut microvilli and other sections of the gut were clearly visualized (Card et al., 2016). Therefore, perhaps the current study required a longer fixation time.

Fuchs et al. (2018) studied *Galleria mellonella* in relation to a bat fungal pathogen, *Pseudogymnoascus destructans,* and a human fungal pathogen, *Pseudogymnoascus pannorum.* After infection, the researchers fixed the larvae in buffered formalin in 4°C for 2 days before processing and staining with H&E. They performed a blind histopathological evaluation on 8 to 9 full-length sagittal larvae sections. Although they did not specify exact organs, they were able to visualize hemocyte nodules forming in response to the fungal pathogens (Fuchs et al., 2018).

In an antibiotic study, Emery et al. (2019) studied *Galleria* in relation to indomethacin, a non-steroidal anti-inflammatory drug that causes gastric ulceration in murine models. Insects were killed and fixed at certain timepoints to evaluate the effects. The larvae were fixed by injection with 100 µL of 10% buffered formalin and then immersed in 10% buffered formalin for 24 h. Larvae were cut into three transverse cross-sections, head, middle, and posterior. The gut organis very clearly imaged with microvilli lining the gut lumen (Emery et al., 2019).

Past studies have concluded that refrigeration of the sample and injection of fixative directly into the insect accelerates the fixation of tissues, as deduced from fixation times described by Card et al. (2016) and Fuchs et al. (2018). In this current study, optimization of the fixative could have increased by keeping larvae fixed for at least two days. A second optimization of midgut pathology would be to dissect it out and fix it separately, as described in Sarwade and Bahwana (2013).

APPENDICES

Appendix A – Amino acid sequence similarity of *Vibrio parahaemolyticus* Pra and Prb to other alike toxins and/or proteins

Pra				
Name	**Length**	**Coverage**	**Identity**	**Accession #**
Vibrio parahaemolyticus	111	100%	100%	WP_023622799.1
Vibrio campbellii	111	100%	99.1%	AYF56253.1
Yersinia intermedia	136	81%	37%	WP_050086265.1
Photorhabdus asymbiotica	133	84%	33.7%	WP_015835800.1
Photorhabdus luminescens	138	84%	33.7%	ABE68878.1
Xenorhabdus beddingii	141	87%	30.9%	WP_086111500.1
Leptinotarsa decemlineata (JHE-related protein)	523	70%	28%	AAC63217.1
Prb				
Name	**Length**	**Coverage**	**Identity**	**Accession #**
Vibrio parahaemolyticus	307	100%	100%	AOS51075.1
Vibrio campbellii	438	100%	100%	AYF56254.1
Yersinia intermedia	416	97%	29.4%	WP_050288781.1
Photorhabdus asymbiotica	419	100%	29.2%	WP_015835799.1
Photorhabdus luminescens	419	100%	29.2%	WP_046395117.1
Xenorhabdus beddingii	424	91%	28.5%	WP_139837448.1
Leptinotarsa decemlineata (JHE-related protein)	523	90%	24.6%	AAC63217.1

Bacillus thuringiensis Cry 2Aa	633	51%	16.7%	AAS75548.1

APPENDIX B – Western Blot Setup

In order to confirm the identity of purified bacterial proteins, a Western Blot was run. The Western Blot gel was moved to a transfer sandwich. The transfer sandwich was created as follows: 1 10 x 7.5 cm filter paper, 1 gel nitrocellular (PVDF) membrane, 1 Western Blot gel with samples, 1 10 x 7.5 cm filter paper, and a sponge. The apparatus was then closed and moved to the tank. The tank was then filled with 1X Tris/Glycine Buffer until the sandwich was covered. An ice pack was added behind the sandwich apparatus before the electrodes were placed.

APPENDIX C – Dosage calculations for Pra and Prb binary toxins produced by *Vibrio parahaemolyticus*

Recombinant Pra and Prb from GenScript® Bank were synthesized using a bacterial expression system. In order to assess their toxicity, the Pra (U7867FA300-1, first amplicon) and Prb (U7867FA300-2, second amplicon) were combined for the purpose of the experiments. Based on their concentrations, they were diluted following the formula below.

Formula : $[Concentration_{toxin}] * (Volume_{toxin}) = [Concentration_{injection}] * (Volume_{injection})$

Recombinant Pra and Prb Concentration from GenScript® Bank:

[Pra]: 2.36 µg Pra/ 1.00 µL 1X PBS + 10% Glycerol

[Prb]: 1.67 µg Prb/ 1.00 µL 1X PBS + 10% Glycerol

0.1 µg inoculum:

Pra Calculation: [2.36 µg/ 1.00 µL] (V1) = [0.1 µg/ 10 µL] (230 µL); V1 = 1.00 µL Pra

1X PBS to add: 230.0 total µL – 1.0 µL Pra = 229.0 µL 1X PBS

Prb Calculation: [1.67 µg/ 1.00 µL] (V1) = [0.1 µg/ 10 µL] (230 µL); V1 = 1.40 µL Prb

1X PBS to add: 230.0 total µL – 1.4 µL Prb = 228.6 µL 1X PBS

0.5 µg inoculum:

Pra Calculation: [2.36 µg/ 1.00 µL] (V1) = [0.5 µg/ 10 µL] (230 µL); V1 = 4.90 µL Pra

1X PBS to add: 230.00 total µL – 4.9 µL Pra = 225.1 µL 1X PBS

Prb Calculation: [1.67 µg/ 1.00 µL] (V1) = [0.5 µg/ 10 µL] (230 µL); V1 = 6.70 µL Prb

1X PBS to add: 230.0 total µL – 6.7 µL Prb = 223.3 µL 1X PBS

When preparing the 0.1 µg and 0.5 µg dosages, the protein suspensions were prepared 30 min. apart and were left on ice for 2 h to allow their individual Pra and Prb components to bind together. The tubes were then vortexed for 20 sec. and allowed to acclimate to room temperature for 5 min. prior to their injection into the larvae. Tubes were vortexed for 60 sec. immediately before drawn into a syringe for injection.

APPENDIX D - Dosage calculations for *Vibrio parahaemolyticus* toxins isolated from overnight cultures

The 13-028/A3 and the ATCC #17802 purified proteins were used for these experiments. After thawing, the toxins were diluted as explained in Materials and Methods, Section 3.5, except that the 2 h period of leaving the toxin on ice for binding was not needed, as the toxin Pra and Prb components are already bound. Their concentrations were obtained from the Bradford Reagent Concentration, as indicated above (Results, Section 1.2). Details of the calculations are provided below.

Formula: $[Concentration_{toxin}] * (Volume_{toxin}) = [Concentration_{injection}] * (Volume_{injection})$

13-028/A3 Native Protein Concentration : [0.5 µg protein/ 1.0 µL 1X PBS]

0.1 µg inoculum:

[0.5 µg/ 1.0 µL] (V1) = [0.1 µg/ 10 µL] (160.0 µL); V1 = 3.2 µL 13-028/A3 protein

1X PBS to add: 160 – 3.2 µL = 156.8 µL 1X PBS

0.5 µg inoculum:

[0.5 µg/ 1.0 µL] (V1) = [0.5 µg/ 10 µL] (160.0 µL); V1 = 16.0 µL 13-028/A3 protein

1X PBS to add: 160.0 total µL – 16.0 PirAB µL = 144.0 µL 1X PBS

ATCC #17802 Native Protein Concentration: [1.0 µg protein/ 1.0 µL 1X PBS]

0.1 µg inoculum:

[1.0 µg/ 1.0 µL] (V1) = [0.1 µg/ 10 µL] (140 µL); V1 = 1.4 µL ATCC protein

1X PBS to add: 140.0 total µL – 1.4 protein µL = 138.6 µL 1X PBS

0.5 µg inoculum:

[1.0 µg/ 1.0 µL] (V1) = [0.5 µg/ 10 µL] (140.0 µL); V1 = 7.0 µL ATCC protein

1X PBS to add: 140.0 total µL – 7.0 protein µL = 133.0 µL 1X PBS

When preparing each protein's 0.1 µg and 0.5 µg dosages, the protein suspensions were prepared 30 min. apart. The tubes were then vortexed for 20 sec. and allowed to acclimate to room temperature for 5 min. prior to their injection into the larvae. Tubes were vortexed for 60 sec. immediately before drawn into a syringe for injection.

REFERENCES

Abbott, W.S. A method of computing the effectiveness of an insecticide. 1925. *Journal of Economic Entomology*, 18: 265-266.

Ahantarig, A., Chantawat, N., Waterfield, N., Ffrench-Constant, R, and Kittayapong, P. PirAB toxin from *Photorhabdus asymbiotica* as a larvicide against dengue vectors. 2009. *Applied and Environmental Micro.*, 75: 4627-4629.

Andrea, A., Krogfelt, K., and Jenssen, H. Methods and challenges of using the greater wax moth (*Galleria mellonella*) as a model organism in antimicrobial compound discovery. 2019. *Microorganisms*, 7: 85.

Aranguren Caro, F., Hung, M., Noble, B., and Dhar, A. Acute hepatopancreatic necrosis disease (VP_{AHPND}), a chronic disease in *Penaeus vannamei* population raised in Latin America. 2020. *Journal of Invertebrate Pathology*, 174: 107424.

Becnel, J. Complementary techniques: preparations of entomopathogens and diseased specimens for more detailed study using microscopy. 2012. *Elsevier Ltd.*, 451-470.

Blackburn, M., Farrar, R., Novak, N., and Lawrence, S. Remarkable susceptibility of the diamondback moth (*Plutella xylostella*) to ingestion of Pir toxins from *Photorhabdus luminescens*. 2006. *Entomologia Experimentalis et Applicata*, 121: 31-37.

Boemare, N., Akhurst, R., and Mourant, R. Deoxyribonucleic acid relatedness between *Xenorhabdus* spp. (Enterobacteriaceae), symbiotic bacteria of entomopathogenic nematodes, with a proposal to transfer *Xenorhabdus luminescens* to a new genus *Photorhabdus* gen. nov. 1993. *International Journal of Systematic Bacteriology*, 43: 249-255.

Bouklas, T., Diago-Navarro, E., Wang, X., Fenster, M., and Fries, B. Characterization of the

virulence of *Cryptococcus neoformans* strains in an insect model. 2015. *Virulence,* 6: 809-813.

Broberg, C., Calder, T., and Orth, K. *Vibrio parahaemolyticus* cell biology and pathogenicity determinants. 2011. *Microbes Infect,* 13: 992-1001.

Broberg, C., Zhang, L., Gonsales, H., and *et al.* A *Vibrio* effector protein is an inositol phosphatase and disrupts host cell membrane integrity. 2010. *Science,* 329: 1660-1662.

Browne, N., Heelan, M., and Kavanagh, K. An analysis of the structural and functional similarities of insect hemocytes and mammalian phagocytes. 2013. *Virulence,* 4: 597-603.

Burdette, D., Yarbrough, M., Oryedahl, A., and *et al. Vibrio parahaemolyticus* orchestrates a multifaceted host cell infection by induction of autophagy, cell rounding, and then cell lysis. 2008. *Proc. Natl. Acad. Sci. U S A.,* 105: 12497-12502.

Büyükgüzel, E., Tunaz, H., Stanley, D., and Büyükgüzel, K. Eicosanoids mediate *Galleria mellonella* cellular immune response to viral infection. 2007. *J. Insect Physiol.,* 53: 99-105.

Card, R., Vaughan, K., Bagnall, Spiropoulos, J., and *et al.* Virulence characterisation of *Salmonella enterica* isolates of differing antimicrobial resistance recovered from UK livestock and imported meat samples. 2016. *Front Microbiol.,* 7: 640.

Castagnola, A, Mulley, G., Davis, N., Waterfield, N., and Stock, P. Transcript abundance of *Photorhabdus* insect-related (Pir) toxin in *Manduca sexta* and *Galleria mellonella* infections. 2016. *Toxins,* 8: 1-9.

Castagnola, A. and Stock, P. Common virulence factors and tissue targets of entomopathogenic bacteria for biological control of Lepidopteran pests. 2014. *Insects,* 5: 139-166.

Chakroun, M., Banyuls, N., Bel, Y., and *et al*. Bacterial vegetative insecticidal proteins (Vip) from entomopathogenic bacteria. 2016. *American Society for Microbiology,* 80: 329-350.

Champion, O., Wagley, S., and Titball, R. *Galleria mellonella* as a model host for microbiological and toxin research. 2016. *Virulence,* 7: 840-845.

Coleman, J., Muhammed, M., Kasperkovitz, P., and *et al. Fusarium* pathogenesis investigated using *Galleria mellonella* as a heterologous host. 2011. *Fungal Biol.,* 115: 1279-1289.

Crosland, R., Fitch, R., and Hines, H. Characterization of B-leptinotarsin-h and the effects of calcium flux antagonists on its activity. 2005. *Toxicon,* 45: 829-841.

Desalermos, A., Fuchs, B., and Mylonakis, E. Selecting an invertebrate model host for the study of fungal pathogenesis. 2012. *PLoS Pathog.*, 8: e1002451.

Desbois, A. and Coote, P. Wax moth larva (*Galleria mellonella*): An *in vivo* model for assessing the efficacy of antistaphylococcal agents. 2011. *J. Antimicrob. Chemother.*, 66: 1785-1790.

Dhar, A., Piamsomboon, P., Caro, L., and *et al.* First report of acute hepatopancreatic necrosis disease (AHPND) occurring in the USA. 2019. *Dis. Aquat. Org.,* 132: 241-247.

Dong, X., Wang, H., Xie, G., and *et al.* An isolate of *Vibrio campbellii* carrying the pirVP gene causes acute hepatopancreatic necrosis disease. 2017. *Emerg. Microb. Infect.*, 6: e2.

Drake, S., DePaola, A., and Jaykus, L. An overview of *Vibrio vulnificus* and *Vibrio parahaemolyticus*. 2007. *Compr. Rev. Food. Sci. Food Safe,* 6: 120-144.

Duchaud, E., Rusniok, C., Frangeul, L., and *et al.* The genome sequence of the entomopathogenic bacterium *Photorhabdus luminescens*. 2003. *Nature Biotechnology,* 21: 1307-1313.

Ellis, J., Graham, J., and Mortensen, A. Standard methods for wax moth research. 2013. *J. of Apicult. Res.,* 52: 1-17.

Emery, H., Johnston, R., Rowley, A., and Coates, C. Indomethacin-induced gut damage in a surrogate insect model, *Galleria mellonella*. 2019. *Archives of Toxicology*, 93: 2347-2360.

Ffrench-Constant, R., Dowling, A., and Waterfield, N. Insecticidal toxins from *Photorhabdus* bacteria and their potential use in agriculture. 2007. *Toxicon*, 49: 436-451.

Ffrench-Constant, R., Waterfield, N., Burland, V., and *et al.* A genomic sample sequence of the entomopathogenic bacterium *Photorhabdus luminescens* W14: Potential implications for virulence. 2000. *Applied and Environ. Microbio.*, 66: 3310-3329.

Finkelstein, R. Chapter 24: Cholera, *Vibrio cholerae* O1 and O139, and other pathogenic *Vibrios*. Medical Microbiology, 4th edition. 1996. Galveston (TX): University of Texas Medical Branch at Galveston.

Firacative, C., Duan, S., and Meyer, W. *Galleria mellonella* model identifies highly virulent strains among all major molecular types of *Cryptococcus gattii*. 2014. *PLoS ONE*, 9: e105076.

Froelich, B. and Nobel, R. *Vibrio* bacteria in raw oysters: managing risks to human health. 2016. *Philos. Trans. R. Soc. Lond. B. Biol. Sci.*, 371: 1689.

Forst, S., Dods, B., Boemare, N., and Stackebrandt, E. *Xenorhabdus* and *Photorhabdus* spp.: Bugs that kill bugs. 1997. *Annual Review of Microbiology*, 51: 47-72.

Fuchs, B., Chaturvedi, S., Rossoni, R. and *et al. Galleria mellonella* experimental model for bat fungal pathogen *Pseudogymnoascus destructans* and human fungal pathogen *Pseudogymnoascus pannorum*. 2018. *Virulence*, 9: 1539-1547.

Garzon, S., Charpentier, G., and Kurstak, E. Morphogenesis of the nodamura virus in the larvae of the lepidopteran *Galleria mellonella* (L.). 1978. *Arch. Virol.*, 56: 61-76.

Gibson, R. and Barker, P. The decapod hepatopancreas. 1979. *Oceanogr. Mar. Biol.*, 77: 285-346.

Han, J., Tang, K., Aranguren, L., and Piamsomboon, P. Characterization and pathogenicity of acute hepatopancreatic necrosis disease natural mutants, PirABvp (-) *V. parahaemolyticus* and PirABvp (+) *V. campbellii* strains. 2017. *Aquaculture,* 470: 84-90.

Han, J., Tang, K., Tran, L., and Lightner, D. *Photorhabdus* insect-related (Pir) toxin-like genes in a plasmid of *Vibrio parahaemolyticus*, the causative agent of acute hepatopancreatic necrosis disease (AHPND) of shrimp. 2015. *Dis. Aquat. Org.*, 113: 33-40.

Hao, J., Zhang, Y., Fu, S., and *et al.* Pathogenicity and protein analysis of *Photorhabdus* insect-related (Pir) toxin PirAB revealed $PirAB^{vp}$ is a host-specific toxin. 2019. *Aquaculture,* 500: 290-299.

Head, G., Jackson, J., Adamczyk, J., Bradley, J., and *et al.* Spatial and temporal variability in host use by *Helicoverpa zea* as measured by analyses of stable carbon isotope ratios and gossypol residues. 2010. *J. App. Ecol.*, 47: 583-592.

Höfte, H. and Whiteley, H. Insecticidal Crystal Proteins of *Bacillus thuringiensis*. 1989. *Microbiol. Rev,* 53: 242-255.

Hong, X., Lu, L., and Xu, D. Progress in research on acute hepatopancreatic necrosis disease (AHPND). 2016. *Aquacult. Int.,* 24: 577-593.

Ibrahim, M., Griko, N., Junker, M., and Bulla, L. *Bacillus thuringiensis*: A genomics and proteomics perspective. 2010. *Bioeng. Bugs*, 1: 31-50.

Izore, T., Job, V., and Dessen, A. Biogenesis, regulation, and targeting of the type III secretion system. 2011. *Structure,* 19: 603-612.

Jafri, R. and Chaudhry, M. Development of Tipula iridescent virus (TIV) in *Galleria mellonella* larvae exposed to gamma radiation. 1971. *J. Invertebr. Pathol.,* 18: 46-50.

Jorjao, A., Oliveira, L., Scorzoni, L., Figueiredo-Godoi, L., and *et al*. From moths to caterpillars:

Ideal conditions for *Galleria mellonella* rearing for *in vivo* microbiological studies. 2017. *Virulence,* 9: 383-389.

Joyce, S. and Gahan, C. Molecular pathogenesis of *Listeria monocytogenes* in the alternative model host *Galleria mellonella*. 2010. *Microbiology,* 156: 3456-3468.

Kaneko, T. and Colwell, R. Ecology of *Vibrio parahaemolyticus* in Chesapeake Bay. 1973. *J. Bacteriol.,* 113: 24-32.

Kanrar, S. and Dhar, A. Complete Genome Sequence of a Novel Mutant Strain of *Vibrio parahaemolyticus* from Pacific White Shrimp (*Penaeus vannamei*). 2018. *Genome Announc.,* 6(24): e00497-18.

Karunasagar, I., Pai, R., and Malathi, G. Mass mortality of *Penaeus monodon* larvae due to antibiotic-resistant *Vibrio harveyi* infection. 1994. *Aquaculture,* 128: 203-209.

Kodama, T., Gotoh, K., Hiyoshi, H., and *et al.* Two regulators of *Vibrio parahaemolyticus* play important roles in enterotoxicity by controlling the expression of genes in the *Vp*-PAI region. 2010. *PLoS One,* 5: e8678.

Kondo, H., Tinwongger, S., Proespraiwong, P., and *et al*. Draft genome sequences of six strains of *Vibrio parahaemolyticus* isolated from early mortality syndrome/acute hepatopancreatic necrosis disease shrimp in Thailand. 2014. *Genome Announc*., 2: e00221-14.

Kondo, H., Van, P., Dang, L., and Hirono, I. Draft genome sequence of non-*Vibrio parahaemolyticus* Acute Hepatopancreatic Necrosis Disease strain KC13.17.5, isolated from diseased shrimp in Vietnam. 2015. *Genome Announc.*, 3: e00978-15.

Koul, O. Microbial biopesticides: opportunities and challenges. 2011. *CAB Reviews: Perspectives in Agriculture, Veterinary Science, Nutrition and Natural Resources,* 6: 1-26.

Kwadha, C., Ong'amo, G., Ndegwa, P., Raina, S., and Fombong, A. The biology and control of the greater wax moth, *Galleria mellonella*. 2017. *Insects,* 8: 61.

Kumar, R., Ng, T., Chang, C., Lin, S., Lo, C., and Wang, H. Bile acid and bile acid transporters are involved pathogenesis of acute hepatopancreatic necrosis disease in white shrimp *Litopenaeus vannamei.* 2016. *Cellular Microbiology*, 22: e13127.

La Rosa, S., Diep, D., Nes, I., and Brede, D. Construction and application of a luxABCDE reporter system for real-time monitoring of *Enterococcus faecalis* gene expression and growth. 2012. *Appl. Environ. Microbiol*., 78: 7003-7011.

Lee, C., Chena, I., Yanga, Y., Ko, T., and *et al.* The opportunistic marine pathogen *Vibrio parahaemolyticus* becomes virulent by acquiring a plasmid that expresses a deadly toxin. 2015. *PNAS*, 112: 10797-10803.

Letchumanan, V., Chan, K., and Lee, L. *Vibrio parahaemolyticus*: A review on the pathogenesis, prevalence, and advance molecular identification techniques. 2014. *Front Microbiol.,* 5: 705.

Li, Y., Hu, X., Zhang, X., and *et al. Photorhabdus luminescens* PirAB-fusion protein exhibits both cytotoxicity and insecticidal activity. 2014. *FEMS Micro. Letters,* 356: 23-31.

Li, P., Kinch, L., Ray, A., and *et al.* Acute Hepatopancreatic Necrosis Disease-causing *Vibrio parahaemolyticus* strains maintain an antibacterial type VI secretion system with versatile effector repertoires. 2017. *Applied Environ. Microbiol.*, 83: 1-17.

Lightner, D. A handbook of shrimp pathology and diagnostic procedures for diseases of cultured penaeid shrimp. 1996. Baton Rouge (LA): World Aquaculture Society.

Lim, J., Stones, D., Hawley, C., Watson, C., and Krachler, A. Multivalent

adhesion molecule 7 clusters act as signaling platform for host cellular GTPase activation and facilitate epithelial barrier dysfunction. 2014. *PLoS Pathogens,* 10: e1004421.

Lin, S., Chen, Y., Hsu, K., and *et al.* Structural insights to the heterotetrameric interaction between the *Vibrio parahaemolyticus* Pravp and Prbvp toxins and activation of the Cry-like pore-forming domain. 2019. *Toxins,* 11: 1-15.

Lin, S., Hsu, K., and Wang, H. Structural Insights into the Cytotoxic Mechanism of *Vibrio parahaemolyticus* Pravp and Prbvp Toxins. 2017. *Marine Drugs,* 15: 373.

Liu, D., Burton, S., Glancy, T., Li, Z., Hampton, R., Meade, T., and Merlo, D. Insect resistance conferred by 283-kDa *Photorhabdus luminescens* protein TcdA in *Arabidopsis thaliana*. 2003. *Nat. Biotechnol*., 21: 1307-1313.

Loh, J., Adenwalla, N., Wiles, S., and Proft, T. *Galleria mellonella* larvae as an infection model for group A streptococcus. 2013. *Virulence*, 4: 419-428.

Machado, A., Zarfl, C., Rehse, S., and Kloas, W. Low-dose effects: Nonmonotonic responses for the toxicity of a *Bacillus thuringiensis* biocide to *Daphnia magna.* 2017. *Environ. Sci. & Tech.,* 51: 1679-1686.

Mehrotra, M., Singh, A., Sanyal, I., and *et al.* Pyramiding of modified cry1Ab and cry1Ac genes of *Bacillus thuringiensis* in transgenic chickpea (*Cicer arietinum* L.) for improved resistance to pod borer insect *Helicoverpa armigera*. 2011. *Euphytica,* 182: 87-102.

Mai, H., Cruz-Flores, R., and Dhar, A. Development of an indirect enzyme linked immunoassay (iELISA) using monoclonal antibodies against *Photorhabdus* insect related toxins, PirA^{Vp} and PirB^{Vp} released from *Vibrio* spp. 2020. *Journ. of Microbio. Methods,* 176: 106002.

Martin, L., Leclercq, A., Savin, C., and Carniel, E. Characterization of atypical isolates of

Yersinia intermedia and definition of two new biotypes. 2009. *Journ. of Clinical Microbio.*, 47: 2377-2380.

Ng, T., Lu, C., Lin, S., Chang, C., and *et al.* The Rho signaling pathway mediates the pathogenicity of AHPND-causing *V. parahaemolyticus* in shrimp. 2018. *Cellular Microbiology*, 20: e12849.

Nunan, L., Lightner, D., Pantoja, C., and Gomez-Jimenez, S. Detection of acute hepatopancreatic necrosis disease (AHPND) in Mexico. 2014. *Dis. Aquat. Org*., 111: 81-86.

Oerke, E. Crop losses to pests. 2006. *Jounr. of Agricul. Science*, 144: 31-43.

Okada, N., Matsuda, S., Matsuyama, J., and *et al.* Presence of genes for type III secretion system 2 in *Vibrio mimicus* strains. 2010. *BMC Microbiology*, 10: 302.

Palma, L., Munoz, D., Berry, D., Murillo, J., and Caballero, P. *Bacillus thuringiensis* toxins: An overview of their biocidal activity. 2014. *Toxins (Basel)*, 6: 3296-3325.

Paddock, F. The beemoth or waxworm. 1918. College Station (TX): Texas Agricultural Experiment Stations.

Paramasiva, I., Sharma, H., and Krishnayya, P. Antibiotics influence the toxicity of the delta endotoxins of *Bacillus thuringiensis* towards the cotton bollworm, *Helicoverpa armigera.* 2014. *BMC Microbiology*, 14: 200.

Park, K., Ono, T., Rokuda, M., and *et al.* Functional characterization of two type III secretion systems of *Vibrio parahaemolyticus*. 2004. *Infect. Immun.*, 72: 6659-6665.

Park, K., Ono, T., Rokuda, M., Jang, M., Iida, T., and Honda, T. Cytotoxicity and enterotoxicity of the thermostable direct hemolysin-deletion mutants of *Vibrio parahaemolyticus*. 2004. *Microbiol. Immunol.*, 48: 313-318.

Pereira, T., Barros, P., Fugisaki, L., and *et al.* Recent advances in the use of *Galleria mellonella*

model to study immune responses against human pathogens. 2018. *Journal of Fungi*, 4: 1-19.

Perdoni, F., Falleni, M., Tosi, D., Cirasola, D., and *et al.* A histological procedure to study fungal infection in the wax moth *Galleria Mellonella*. 2014. *Eur. J. Histochem.,* 58: 2428.

Pimentel, D., Zuniga, R., and Morrison, D. Update on the environmental and economic costs associated with alien-invasive species in the United States. 2005. *Ecological Economics*, 52: 273-288.

Punsalang, A., Edinger, R., and Nolte, F. Identification and characterization of *Yersinia intermedia* isolated from human feces. 1987. *Jounr. of Clinical Microbio.,* 25: 859-862.

Restrepo, L., Bayot, B., Arciniegas, S., and *et al.* PirVP genes causing AHPND identified in a new *Vibrio* species (*Vibrio punensis*) within the commensal *Orientalis* clade. 2018. *Scientific Reports*, 8: 13080.

Rezny, B. and Evans, D. *Vibrio parahaemolyticus*. 2019. Treasure Island (FL): StatPearls Publishing.

Rohrmann, G. Baculovirus. Molecular Biology, 4th edition. 2019. Bethesda (MD): National Center for Biotech Information.

Roush, R. Two-toxin strategies for management of insecticidal transgenic crops: Can pyramiding succeed where pesticide mixtures have not? 1998. *Philos. Trans. R. Soc. Lond. B. Biol. Sci.*, 353: 1777-1786.

Sarwade, A. and Bhawane, G. Anatomical and histological structure of digestive tract of adult *Platynotus belli.* F (Coleoptera: Tenebrionidae). 2013. *Biological Forum,* 5: 47-55.

Schnepf, E., Crickmore, N., Rie, J., and *et al. Bacillus thuringiensis* and its pesticidal crystal

proteins. 1998. *Micro. and Molec. Bio. Rev.*, 62: 775-806.

Scorzoni, L., de Paula e Silva, A., Singulani, J., Leite, F., and *et al.* Comparison of virulence between *Paracoccidioides brasiliensis* and *Paracoccidioides lutzii* using *Galleria mellonella* as a host model. 2015. *Virulence*, 6: 766-776.

Shimanuki, H. Diseases and pests of honeybees. Volume 335: Bee keeping in the United States. 1980. Washington DC (WA): Science and Education Administration, United States Department of Agriculture, pp. 118-128.

Slater, J., Gregson, L., Denning, D., and Warn, P. Pathogenicity of *Aspergillus fumigatus* mutants assessed in *Galleria mellonella* matches that in mice. 2011. *Med. Mycol.*, 49: S107-S113.

Sirikharin, R., Taengchaiyaphum, S., Sanguanrut, P., and *et al.* Characterization and PCR detection of binary, Pir-like toxins from *Vibrio parahaemolyticus* isolates that cause Acute Hepatopancreatic Necrosis Disease (AHPND) in shrimp. 2015. *PLoS One*, 10: e0126987.

Tanet, L., Tamburini, C., Baumas, C., and *et al.* Bacterial bioluminescence: Light emission in *Photobacterium phosphoreum* is not under quorum-sensing control. 2019. *Front. Microbiol.*, 10: 365.

Thomaz, L.,García-Rodas, R., Guimarães, A., Taborda, C., and *et al. Galleria mellonella* as a model host to study *Paracoccidioides lutzii* and *Histoplasma capsulatum*. 2013. *Virulence*, 4: 139-146.

Tran, L., Nunan, L., Redman, R., and *et al.* Determination of the infectious nature of the agent of acute hepatopancreatic necrosis syndrome affecting penaeid shrimp. 2013. *Dis. Aquat. Organ.*, 105: 45-55.

Tsai, C., Loh, J., and Proft, T. *Galleria mellonella* infection models for the study of bacterial diseases and for antimicrobial drug testing. 2016. *Virulence*, 7: 214-229.

Tseng, T., Tyler, B., and Setubal, J. Protein secretion systems in bacterial-host associations, and their description in the Gene Ontology. 2009. *BMC Microbiol.*, 9: S2.

Vermunt, A., Koopmanschap, A., Vlak, J., and Kort, C. Cloning and sequence analysis of cDNA encoding a putative juvenile hormone esterase from the Colorado potato beetle. 1997. *Insect Biochem. Molec. Biol.*, 27: 919-928.

Victorio-De Los Santos, M., Perez-Vibanco, N., Rodriguez, S., Pereyra, A., and *et al*. The B subunit of PirAB^{vp} toxin secreted from *Vibrio parahaemolyticus* causing AHPND is an amino sugar specific lectin. 2020. *Pathogens,* 9: 182.

Vlisidou, I., Hapeshi, A., Healey, J., and *et al.* The *Photorhabdus asymbiotica* virulence cassettes deliver protein effectors directly into target eukaryotic cells. 2019. *Elife,* 8: e46259.

Wagley, S., Borne, R., Harrison, J., and *et al. Galleria mellonella* as an infection model to investigate virulence of *Vibrio parahaemolyticus.* 2018. *Virulence,* 9: 197-207.

Wang, S., Kain, W., and Wang, P. *Bacillus thuringiensis* Cry1A toxins exert toxicity by multiple pathways in insects. 2018. *Insect Biochem. Mol. Biol.*, 102: 59-66.

Waterfield, N., Ciche, T., and Clarke, D. *Photorhabdus* and a host of hosts. 2009. *Annual Review of Microbiology,* 63: 557-574.

Waterfield, N., Hares, M., and Yang, G. Potentiation and cellular phenotypes of the insecticidal toxin complexes of *Photorhabdus* bacteria. 2005. *Cell. Microbiol.*, 7: 373-382.

Waterfield, N., Kamita, G., Hammock, B., and Ffrench-Constant, R. The *Photorhabdus* Pir toxins are similar to a developmentally regulated insect protein but show no juvenile hormone esterase activity. 2005. *FEMS Microbio. Letters,* 245: 47-52.

Williamson, D., Mills, G., Johnson, J., Porter, S., and Wiles, S. *In vivo* correlates of molecularly

inferred virulence among extraintestinal pathogenic *Escherichia coli* (ExPEC) in the wax moth *Galleria mellonella* model system. 2014. *Virulence*, 5: 388-393.

Wittwer, D., Franchini, A., Ottaviani, E., and Wiesner, A. Presence of IL-1- and TNF-like molecules in *Galleria mellonella* (Lepidoptera) haemocytes and in an insect cell line *Fromestigmene acraea* (Lepidoptera). 1999. *Cytokine*, 11: 637-642.

Wu, G. and Yi, Y. Haemocoel injection of Pra1B1 to *Galleria mellonella* larvae leads to disruption of the haemocyte immune functions. 2016. *Sci. Reports,* 6: 1-7.

Xiao, J., Liu, L., Ke, Y., and *et al.* Shrimp AHPND-causing plasmids encoding the PirAB toxins as mediated by pirAB-Tn903 are prevalent in various *Vibrio* species. 2017. *Scientific reports,* 7: 42177.

Yang, Q., Zhang, J., Li, T., and *et al.* PirAB protein from *Xenorhabdus nematophila* HB310 exhibits a binary toxin with insecticidal activity and cytotoxicity in *Galleria mellonella.* 2017. *Journ. of Invertebrate Path.,* 148: 43-50.

Zhang, X., Hu, X., Li, Y., Ding, X., and *et al.* XaxAB-like binary toxin from *Photorhabdus luminescens* exhibits both insecticidal activity and cytotoxicity. 2014. *FEMS Microbiol. Lett.,* 350: 48-56.

Zhao, J., Cao, J., Collins, H., and *et al.* Concurrent use of transgenic plants expressing a single and two *Bacillus thuringiensis* genes speeds insect adaptation to pyramided plants. 2005. *Proc. Natl. Acad. Sci. U. S. A.,* 102: 8426-8430.

Zhao, J., Cao, J., Collins, H., and *et al.* Transgenic plants expressing two *Bacillus thuringiensis* toxins delay insect resistance evolution. 2003. *Nat. Biotechnol.,* 21: 1493-1497.